Exploring the Potential of Artificial Intelligence in Healthcare: ECG Reconstruction from Single Lead ECG Recordings and PPG Signals

Thesis submitted in partial fulfilment
of the requirements for the degree of

Master of Science
in
Computational Natural Sciences by Research

by

Akshit Garg
2018113006
akshit.garg@research.iiit.ac.in

International Institute of Information Technology
Hyderabad - 500 032, INDIA
June 2023

International Institute of Information Technology
Hyderabad, India

CERTIFICATE

It is certified that the work contained in this thesis, titled "Exploring the Potential of Artificial Intelligence in Healthcare: ECG Reconstruction from Single Lead ECG Recordings and PPG Signals" by Akshit Garg, has been carried out under my supervision and is not submitted elsewhere for a degree.

Date

Advisor: Prof. U. Deva Priyakumar

To MY FAMILY
& FRIENDS.

Acknowledgments

I would like to express my heartfelt appreciation to my research advisor, Dr. U Deva Priyakumar, for his unwavering support and guidance throughout my research work. His precise feedback and enthusiasm towards research have been a great inspiration to me. I am deeply grateful for Dr. Vinod P. K.'s valuable support and guidance in the studies related to COVID-19. Working with both of them has been an enriching experience that I truly appreciate.

My research journey has been shaped by the valuable contributions and insightful discussions of Vijay, Abhiroop, and Bhuvanesh. They have played a significant role in shaping my work, and I cannot thank them enough for their guidance and support. I also extend my thanks to my seniors Manan, Akshaya, and Shanmukh, who have always been there to provide guidance and support whenever I needed it. I am also thankful to all the members of the DevaLab for creating a supportive and collaborative environment that has facilitated my research work.

I would like to express my heartfelt gratitude to my friends at IIIT Hyderabad, including Anubhav, Aryamaan, Guru, Jashn, Kushagra, Manas, Nikunj, Sajal, Satyam, and Shantanu. They have made my life wonderful over the past few years, providing unwavering support and companionship that have been a constant source of motivation. Their willingness to listen and support me during difficult times has been invaluable. I am truly grateful for their friendship and the memories we have shared together.

Above all, I am immensely grateful to my loving and supportive family, especially my parents and brother, for their unwavering encouragement and affection throughout my life. Their constant love and support have been the foundation of my success, and I am deeply indebted to them.

Abstract

In the recent years we have seen an enormous increase in the utilisation of Artificial Intelligence (AI), and the healthcare sector has not been exempt from this transformation. Machine learning systems have demonstrated unmatched success in the healthcare sector thanks to recent developments in digitalization and the massive influx of biomedical data. This could be a game changer for the sector. The rise of cardiovascular diseases across the globe has made electrocardiograms (ECGs) a crucial modality for diagnosis, owing to their non-invasive nature and simplicity. However, gathering 12-lead ECG data is an arduous task outside clinical settings. Wearables can collect an ECG with fewer leads than the standard 12 or the Photoplethysmogram (PPG) data, but medical professionals and conventional ECG analysis software find this data challenging to interpret. To address this issue, ECG reconstruction has been proposed.

The second chapter provides a summary of the current applications of AI in diagnosis, prognosis, and therapy, along with its implications for combating the COVID-19 pandemic. The chapter also identifies obstacles to AI's widespread adoption in the healthcare sector and suggests remedies to help usher in a more intelligent medical future.

A unique single-lead to multi-lead ECG reconstruction method is suggested in the third chapter of this thesis employing a modified Attention U-Net framework. Our model, which was solely trained on lead II of ECG, is capable of replicating the remaining 11 leads of the conventional 12-lead ECG with a Pearson correlation of 0.805, a mean square error of 0.0122, and an R-squared value of 0.639. Moreover, a single combined model is used to reconstruct all 11 leads simultaneously, improving performance and simultaneously reducing the computational resources needed for training compared to current literature in the field. The model's ability for real-life use was also demonstrated by training a deep learning model for multi-disease classification using actual 12-lead ECG data and testing it on both original and reconstructed 12-lead ECG signals. Comparable classification accuracies for both original and reconstructed signals suggest that the proposed model can preserve diagnostically relevant artefacts.

The fourth chapter proposes a new approach using a Wasserstein generative adversarial network to convert PPG signals into single lead ECG signals. Unlike previous studies, we utilize longer 3-second PPG segments to generate a complete 3-second ECG signal in a single step. We also address a signif-

icant issue in earlier studies where same patient's data was used for both model training and testing. To address this limitation, patient-specific data segmentation for the train and test set was employed to obtain more reliable results.

In summary, this thesis proposes solutions for multi-lead ECG reconstruction and PPG to ECG conversion, aiming to bridge the divide between easily collected heart monitoring data and easily interpretable heart monitoring data.

Contents

List of Figures

List of Tables

Chapter 1

Introduction

The healthcare industry is undergoing a significant transformation with the integration of artificial intelligence (AI), which is revolutionizing the way medical practitioners diagnose, treat, and prevent diseases. The shortage of medical personnel has made it challenging for the healthcare sector to cater to the needs of the growing population [112], prompting the implementation of AI solutions to address this issue. AI technology can aid physicians in diagnosing and predicting diseases, facilitating quick and efficient decision-making. The digitization of medical records has opened up access to vast amounts of data previously unavailable, which has helped in the creation of novel AI solutions. Due to the high influx of biomedical data, machine and deep learning studies are presently dominant in the AI healthcare industry. These studies can be applied to existing medical practices, providing solutions to the challenges faced by the healthcare industry. As the healthcare sector continues to evolve, AI integration is likely to play an essential role in improving patient outcomes and enhancing the overall quality of care.

Cardiology is a crucial field in medicine that deals with the prevention, diagnosis, and treatment of various heart-related conditions.The heart is a vital organ that circulates blood throughout the body, playing an important role in the proper functioning of the circulatory system. Cardiovascular diseases, including coronary heart disease, heart failure, and arrhythmia, are significant health concerns globally, and they are a leading cause of mortality. The World Health Organization (WHO) has estimated that around 17.9 million people die from cardiovascular diseases annually. The management of many diseases depends on early identification and prompt action, and AI has demonstrated considerable promise in this area [73, 37]. AI has been used in cardiology for a variety of applications, including the analysis of medical images, electrocardiogram (ECG) signals, and blood parameters to detect anomalies and identify potential cardiovascular diseases. AI algorithms can assist physicians in the diagnosis and treatment of cardiac conditions by providing more accurate and efficient analyses of patient data [53, 99, 130, 115, 151, 3, 145]. Additionally, AI can help predict patient outcomes and determine the most suitable treatment options for individual patients based on their medical history, genetics, and other factors [93, 36]. With the integration of AI in cardiology, medical professionals can provide more personalized and effective care to patients, potentially leading to better health outcomes and reduced healthcare costs.

The healthcare industry commonly employs electrocardiogram (ECG) as a non-invasive diagnostic tool for monitoring heart activity. It is a fast and effective method to detect heart-related problems such as arrhythmia, myocardial infarction, and other cardiac conditions [78, 124].To capture the electrical activity produced by the heart, electrodes are positioned in designated spots on the patient's skin during the procedure. The collected signals are then processed and presented to the clinician for further diagnosis. The most commonly used ECG is the 12-lead ECG [105], which requires ten electrodes comprising four limb electrodes and six pre-cordial electrodes. However, precise placement of these electrodes is crucial as even small errors can result in the production of unwanted artefacts in the signals, leading to a possibility of an erroneous diagnosis [101]. Inaccurate diagnosis due to misinterpretation of artefacts is a significant issue, as highlighted in a study by Knight et al. [66]. Moreover, the need for ten electrodes creates a lot of trouble for patients who require continuous monitoring. Consequently, there is a need for further research in the development of a more accurate, easy-to-use, and portable ECG device that requires fewer electrodes for continuous monitoring of patients.

Reduced set ECG and photoplethysmography (PPG) are easier to collect than the 12-lead ECG, and can be used to obtain a picture of cardiac conditions. Reduced set ECGs use fewer electrodes than the 12-lead variant, making it easier and quicker to set up. In contrast, PPG measures changes in blood volume through the skin using a non-invasive optical technique. It can be measured using a simple finger clip, making it a more convenient option for continuous monitoring compared to ECGs. Both reduced set ECG and PPG have been shown to have good potential for detecting cardiac conditions and anomalies, making them useful tools for screening and monitoring. However, it should be noted that they may not be as accurate as the 12-lead ECG, particularly in diagnosing certain types of cardiac abnormalities.

Despite reduced lead set ECG and PPG data being easier to collect, conventional medical infrastructure is heavily dependent on the 12-lead ECG. This creates a gap between the ease of collecting data and the ability to process it. We offer a Deep Learning-based solution to this problem that produces 12-lead ECG data from single-lead ECG and single-lead ECG data from PPG signals. This thesis involves two main contributions: (1) a Deep Learning architecture to reconstruct 12-lead ECG data using single-lead ECG data, and (2) a method to generate single-lead ECG signals using PPG data. It is essential to note that both methods do not introduce any new information to the input data but rather convert one form of heart monitoring data to another form that is more interpretable by medical practitioners. Our proposed solution aims to improve the accessibility and accuracy of cardiac monitoring, ultimately leading to better healthcare outcomes.

1.1 Organisation of Thesis

- **Chapter 2** of this dissertation provides an overview of the significant advancements that AI has brought to the healthcare industry. The chapter delves into the impact of AI in different fields of healthcare, including Cardiology, Pulmonology, Dermatology, Neurology and Psychiatry, and Oncology. The chapter explores how AI has contributed to medical diagnosis, prognosis and treatment, as well as its crucial role in managing the COVID-19 pandemic. In addition to highlighting the benefits of AI, the chapter acknowledges the challenges that AI faces in the healthcare industry and discusses potential ways to overcome them. This chapter aims to present a thorough overview of the state of AI in healthcare today and its promise in the future.

- **Chapter 3** discusses deep learning methods to reconstruct 12-lead ECG using a single-lead of the ECG.Our proposed solution involves utilizing a modified Attention U-Net framework to reconstruct multi-lead ECG signals from a single lead. Further, a single combined model is used to reconstruct all 11 leads simultaneously, improving performance and simultaneously reducing the computational resources needed for training compared to current literature in the field. In comparison to previous works, which only reconstruct small ECG segments, our model is trained to reconstruct longer 10-second ECG signals. We also demonstrate our model's ability for real-life utilisation using a cardiovascular disease classification task.

- **Chapter 4** of this thesis proposes a novel approach using a Wasserstein generative adversarial network to convert PPG signals into single lead ECG signals. In contrast to previous studies, we utilise longer 3-second PPG segments to generate a complete 3-second ECG signal in a single step. The chapter also highlights a significant issue in earlier studies, where identical patient data was used for both model training and testing. To address this limitation, patient-specific data segmentation was employed to obtain more reliable results.

- **Chapter 5** summarises the work presented in the previous chapters and discusses possible ways to improve the work in future.

Chapter 2

Opportunities and Challenges of Modern AI/ML Methods in Healthcare

2.1 Introduction

In basic terms, AI is a branch of computer science that strives to generate systems that are capable of learning and reasoning just like humans. Even though the idea of AI has been around for a long time, the term "Artificial Intelligence" was first coined in 1956 at a conference in Dartmouth College [109]. Over the past few years, advances in computer hardware, methods, libraries, and datasets have given AI a considerable boost and allowed it to permeate a variety of fields. With the digital revolution, the generation of big datasets has been made possible, leading to the significant success of the data-hungry AI techniques of Machine Learning (ML) and Deep Learning (DL).

The healthcare sector, in particular, is responsible for the maintenance and improvement of health for the people through various means like prevention, diagnosis, treatment and cure of illness (both mental and physical). But with the industry facing a severe shortage of medical staff [112] to treat an ever growing population, this becomes a very challenging task. The advent of AI into the industry can help physicians, assisting them in difficult areas like diagnosis, prognosis and help them make decisions quickly and efficiently. As various hospital records get digitised, researchers have seen a sharp increase in the amount of viable data that can be used for AI, which has been a severely limiting factor in the past. Due to this high influx of biomedical data, AI in healthcare is currently being dominated by ML and DL. Researchers can now use Machine/Deep learning studies and apply them to existing medical practices to come up with innovative solutions to solve issues faced by the healthcare industry. Multimodal data plays an important role in success of AI in Healthcare. Figure 2.1 shows how AI utilizes data from different modalities to assist in various sectors of healthcare. This Chapter will examine a few uses of AI in the areas of diagnosis, prognosis, and treatment in the medical field. We will also look into how AI has played a pivotal role in the COVID-19 pandemic. Finally, we'll talk about some of the difficulties AI in healthcare faces and how to get over them to advance towards a more advanced and smarter medical future.

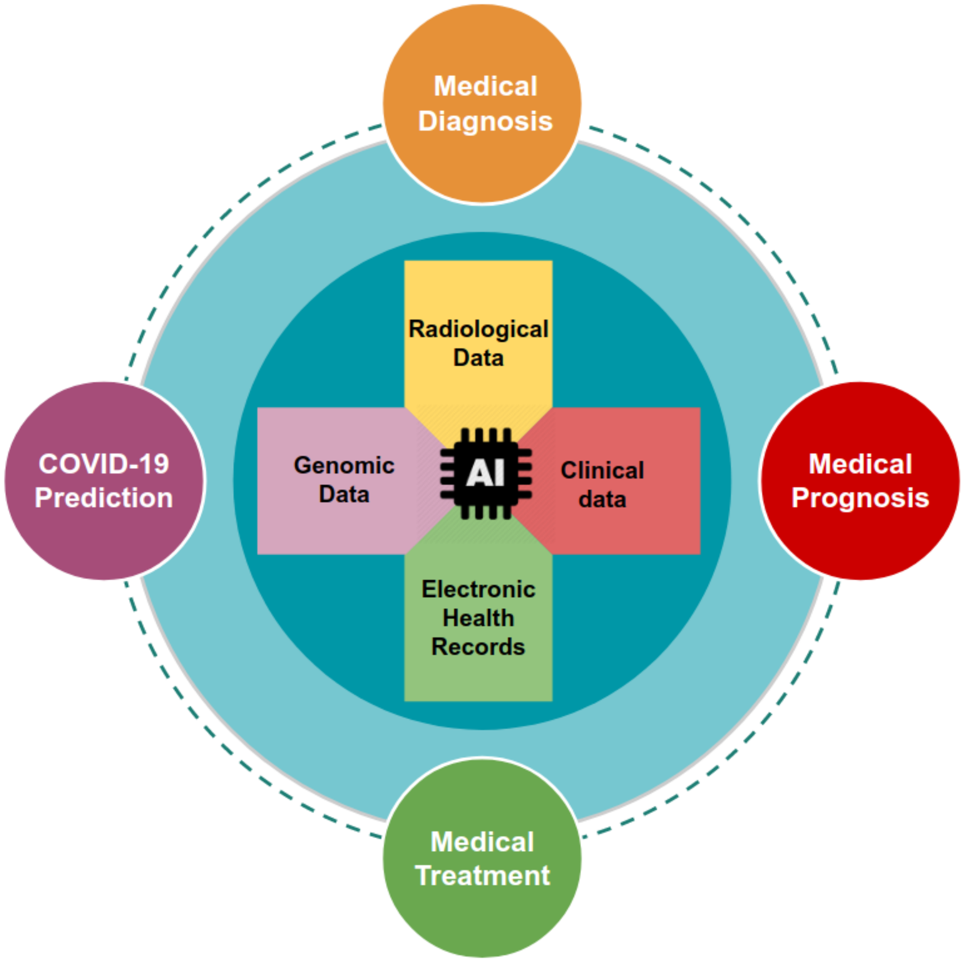

Figure 2.1: A schematic of use of multimodal data and AI for different aspects of healthcare problems.

2.2 AI in Medical Diagnosis

One of the essential steps for providing good medical care is to identify the underlying disease. Diagnosis refers to this process of assessing and identifying the underlying condition from the patient's symptoms. To make an accurate diagnosis, medical professionals may use a variety of techniques, including the patient's medical history, imaging tests, blood testing, etc. ML and DL, in particular, have revolutionised the field of Medical Diagnosis and one can argue that the applications of AI in Diagnosis are the most wide-ranging and successful. In the following section, we will summarize the advances of AI in various medical fields.

2.2.1 Cardiology

Cardiology refers to the branch of medicine that involves studying and treating conditions affecting the heart and circulatory system. Cardiovascular diseases (CVDs) are one of the leading causes of global

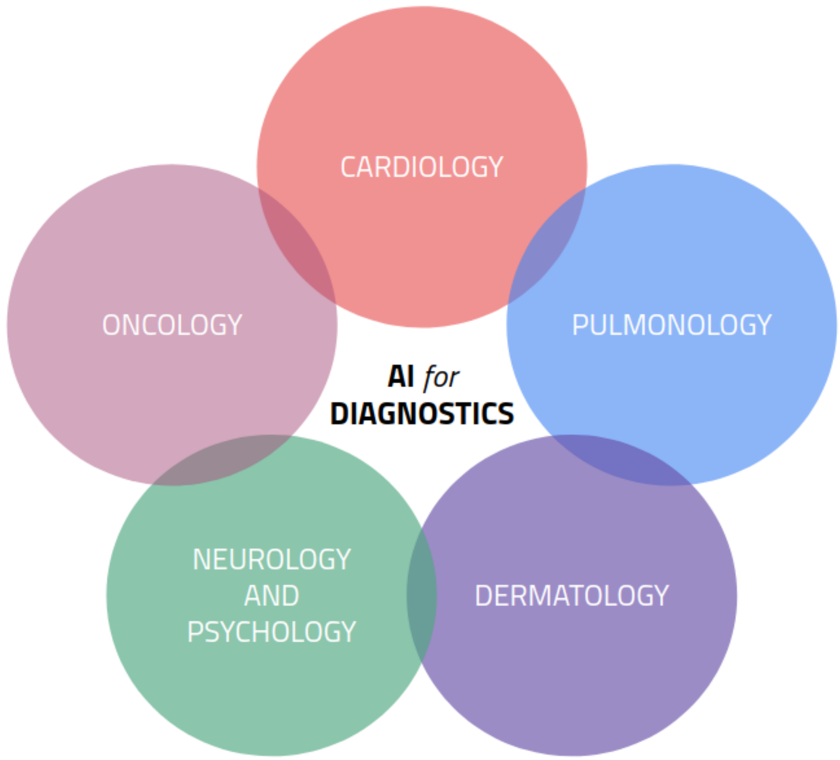

Figure 2.2: Five major medical domains where modern AI/ML methods have been used for disease diagnosis

deaths, leadind to millin of death annually. Through the anomaly identification in cardiac imaging, ECG signals, and blood parameters, various AI applications have been created to assist in the timely detection of different heart problems.

Hussain et al. [53] proposed Linear Kernel Support Vector Machine which analysed the heart rate variability signals to detect Congestive Heart Failure with an area under the receiver operating characteristic curve (AUC) of 0.97. Qu et al. [99] proposed ML methods to detect congestive heart failure with an accuracy of 84.0%. Than et al. [130] introduced an ML algorithm MI^3 which used Gradient boosting to generate a score suggesting probability of Myocardial Infarction (MI). MI^3 was trained on a cohort of 3013 patients and used the combination of clinical data and high-sensitivity cardiac troponin I concentrations to detect MI. Sharma et al. [115] proposed an ML model which utilised the full length multilead ECG signal to detect MI with an AUC of 0.9945 while Weiss et al [151] utilised Statistical Relation Learning Algorithms to detect MI from Electronic Health Records. Akella et al [3] developed a Neural Network using a cohort of 303 patients to detect Coronary Artery Disease (CAD) with an accuracy of 93% using 14 different medical parameters. Wang et al [145] used Random Forest Classifier to detect CAD with an AUC of 0.948.

2.2.2 Pulmonology

Pulmonology is the domain of medicine which deals with the treatment of diseases affecting the respiratory system. Respiratory diseases negatively affect a large part of the global population. Chronic obtructive pulmonary disease(COPD) is a deadly disease which has killed over 3.2 million people in 2019 according to WHO. Early detection of respiratory diseases is an essential step for efficient medical treatment. AI has shown promise in playing a significant role in the timely detection of respiratory diseases [125, 94, 121, 103].

An interesting application of AI to detect COPD using saliva samples was introduced by Zarrin et al [158]. The authors used biosensors to detect the dielectric properties of the saliva samples. The eXtreme Gradient Boosting (XGBoost) algorithm based model is then trained upon these properties to detect the presence of COPD with an accuracy of 91.25%. Porieva et al [98] used a dataset of 296 lung sounds representing 3 classes of normal, bronchitis and COPD. To detect bronchitis and COPD, they collected various variables from the sound recordings and combined them with ML models to achieve an overall accuracy of 93%. Advancements in computer vision and deep learning have led to the creation of models capable of detecting diseases such as pneumonia [131], pulmonary arterial hypertension [126], and pulmonary fibrosis [29] through the analysis of various types of chest imaging.

2.2.3 Dermatology

Dermatology is the branch of medicine involving the study and treatment of skin, hair and nails. Visual inspection is one of the essential steps in diagnosing a dermatological problem. The advancements of computer vision has opened up new horizons for the field of AI in dermatology and have led to some of the recent DL models which can provide a diagnosis which is at par with some of the field's leading experts [133, 41]. With the help of AI, mobile devices can provide easy and cheap access to high-quality medical diagnosis to the parts of population who were previously left behind [135, 22].

A Convolutional neural network (CNN) was trained by Kim et al. [63] using clinical images belonging to 90 different patients. The CNN showcased remarcable performce with identification ability comparable to that of 5 dermatologists. EczemaNet [92] is a CNN trained on clinical images to predict the severity and presence of Atopic Dermatitis with a high accuracy. Gustafson et al. [50] proposed a Natural Language Processing (NLP) based algorithm for Electronic Health Record based phenotyping to identify Atopic Dermatitis in adults. Ros-Net [18] is an Inception-ResNet-v2 trained to detect rosacea with an accuracy of 89.8%. AI based solutions for diagnosis of Psoriasis [136], Onychomycosis [63] are also being proposed. Recent advancements in AI in Dermatology will improve the overall well being of global population.

2.2.4 Neurology and Psychiatry

Neurology is the science of treating and diagnosing the diseases of the nervous system. Early detection of neurological diseases can help in improvement of provided medical care. AI plays an important role in early detection of neurological disorders [113, 128, 8, 85, 33, 123, 107]. Recent studies have aimed for early detection of neurodegenerative diseases using non-coding RNAs and MicroRNAs [74, 38, 75, 160]. AI solutions for timely identification of Alzheimer's disease using Electroencephalography (EEG) [118, 134] are also being put forward. To identify Alzheimer's illness, Liu et al. [71] presented a novel approach that extracts spectrogram characteristics from speech data. Recent studies have tried to exploit gait for early detection of Parkinson's disease [6, 14]. Several DL based solutions have also been proposed which can help in accurate and precise detection of brain hemorrhage in brain CT images [19, 57]. Dammu et al [32] developed an ML model to classify Autism Spectrum Disorder with an accuracy of 73.6% using the resting state functional magnetic resonance imaging (rs-fMRI).

Psychiatry is the branch of medicine associated with the prevention, treatment and diagnosis of mental disorders. Diagnosis of mental illness is an inaccurate and challenging process where a psychiatrist or psychologist tries to evaluate a patients mental health. A large part of the global population does not have access to good psychiatric diagnosis. WHO estimates depression alone affects 5% of the worldwide population, and early detection of depression can make enormous improvements in its medical treatment. AI based depression detection models are being deployed, which use NLP and emotion detection to detect potential patients of depression from their social media feeds [55, 35, 89, 7]. Sato et al. [110] developed ML model to detect people susceptible to major depression using the functional magnetic resonance imaging (fMRI) data. Schizophrenia (SCZ) affects 20 million people worldwide and early detection can help in providing patients with better medical care. ML and DL models are being developed to detect SCZ using the EEG signals [159, 25], genomic data [132] and fMRI data [122] for early and accurate detection of SCZ.

2.2.5 Oncology

In 2018, cancer was responsible for one in six deaths and was the second biggest cause of death across the globe. Oncology is the branch of medicine associated with the treatment of cancer. The potential of AI to facilitate early and precise diagnosis of cancer is considerable. Mobile devices equipped with AI can provide cheap and easy access to remote population [40]. Esteva et al [41] trained a deep CNN on a dataset comprising of 129,450 images to detect skin cancer. The CNN was able to achieve performance comparable with 21 Dermatologists. DL models are being proposed which can detect and classify brain cancer [139, 23], breast cancer [62, 137] and renal cancer [127] from radiological and histopathological images. Whole genome sequencing data is also being used to train ML models which can enable early detection of different cancers [144, 26].

2.3 AI in Medical Prognosis

Health care providers determine a patient's prognosis after correctly diagnosing their underlying disease. Medical prognosis is the process of anticipating or projecting the expected course of a medical condition for a specific patient, including possible outcomes. Given all of the variables, determining an accurate prognosis can be quite challenging. To make an appropriate prognosis, healthcare practitioners consider elements such as patient's medical history, patient's current physiological symptoms and the development path of the disease. Healthcare practitioners' prognosis accuracy and confidence have significantly increased as a result of recent breakthroughs in ML and DL. We go into further detail on how AI has aided prognosis prediction in various research in subsequent subsections.

2.3.1 Cancer Progression Studies

Once a patient is diagnosed with cancer, determining a suitable prognosis is very important as it helps determine the next course of action medically. Cancer is estimated to affect 1 in 10 people on average in the USA [116], making the task of predicting cancer progression very important. Nie et al. [87] proposed a 3 dimensional DL framework for automatic feature extraction from pre-operative multi-modal images like DTI of patients with brain tumors, MRI, fMRI achieving accuracies as high as 89.9%. CNNs are being used to segment a brain tumor from healthy tissue, once the tumor data is extracted, regression is used to predict the time left for survival [54]. Boeri et al. [20] built an ML model to predict outcomes after surgery for breast cancer patients with an accuracy of 95%. Using various deep learning techniques, survival prediction for lung cancel is being predicted with good accuracy [68, 157]. Tang et al. [129] proposed an approach for predicting prognosis of Kidney renal clear cell carcinoma (KIRC). A prognostic model based on genes that are influenced by methylation was developed using lasso regression. Following the prediction of patient survival rates using clinical data and the methylation prognostic model, the test data's C-index value was determined to be 0.838. Instead of targeting a specific type of cancer, there has been research using multi-modal data for pan-cancer prognosis. These papers make use of DL techniques on histopathology slides and other clinical information to finally predict single cancer and pancancer overall survival.[117, 27]

2.3.2 Mortality Prediction Studies

Mortality prediction is the task to forecast the risk of death for a critically ill patient. Building a reliable mortality predictor with AI can help doctors identify critically ill patients, who can then be given special medical attention.

Kong et al. [67] were able to use ML for mortality prediction of ICU patients with sepsis with moderate success. They built four different kinds of machine-learning based classifier models and trained them on the medical information mart for intensive care (MIMIC) III dataset.They found the gradient boosting machine (GBM) gave best AUC of 0.845. Parikh et al. [95] accurately predicted 6-month mortality for cancer patients using gradient boosting and achieved an AUC of 0.87. Studies of mortality prediction is also being done for different kinds of cancer specifically like advanced hepatocellular carcinoma (HCC) [76] and metastatic colorectal cancer (mCRC) [108].

The need for calculating mortality risk for traumatic patients admitted to the ICU is very high, Servia et al. [114] conducted a series of experiment using the RETRAUCI database which has the data of 52 Spanish ICUs during the years between 2015 and 2019. Nine distinct ML models were created, utilizing a set of variables based on deviations in physiological and anatomical parameters, to forecast the risk of mortality for a traumatized patient. Elderly trauma patients generally have a very high risk or mortality, Morris et al. [84] present a set of novel outcome scores, quick elderly mortality after trauma (qEMAT) score and a full elderly mortality after trauma (fEMAT) score, for predicting mortality of elderly trauma patients. They achieve an AUC of 0.84 for the qEMAT and 0.86 for fEMAT.

Stillbirth is the fetal death after 20 or 28 weeks of pregnancy. It is a devastating outcome which accounts to two-thirds of perinatal mortality or live-born children who are yet to complete 7 days of life. [83, 42] Combining elements such as present pregnancy complication, maternal traits and medical history researchers were able to use regularised logistic regression, decision tree, neural network , extreme gradient boosting and random forest which could predict the risk of stillbirth with mild success. 45% of stillbirths among all the women in the dataset could be predicted by the top classifier, XGBoost.[81]

Mortality prediction studies in the field of cardiology has been very active, as cardiovascular diseases account for a large amount of deaths worldwide. Adler et al. [1] developed a boosted decision tree model using data from 5,822 patients hospitalized with heart failure (HF). Using eight key variables the model was able to give a risk score with an AUC of 0.88. Wang et al. [150] introduced a DL system for predicting mortality due to heart failure, the system was invariant to feature rearrangement and was able to handle the imbalanced dataset very well. After 2019, enormous research on the risk stratification and death prediction for COVID-19 patients have been reported; these studies are discussed further.

2.4 AI in Medical Treatment

In the previous sections we discussed how AI has greatly impacted the way healthcare professionals accurately diagnose and give prognosis to patients. In this section, we will look at how AI techniques like ML and DL have helped improve the quality of the treatment they provide to their patients.

Developing emergency department (ED) prioritisation systems capable to assess patients' requirements and conditions to evaluate their care is still a challenging task. Raita et al.[100] were able to build a deep neural network to predict if patients coming to the ED were critically ill with an AUC of 0.86. As the major cause of morbidity, CVDs have a very short window of opportunity, particularly if the patient is hospitalised to the ED. Researchers utilized ML models, such as random forest, extreme gradient boosting, multinomial logistic regression, and gradient-boosted decision tree, to analyze data from approximately 17,661 patients in the emergency department who were suspected of having cardiovascular diseases. They achieved AUC of 0.937 for XGBoost, 0.921 for gradient-boosted decision tree, 0.919 for random forest and 0.908 for multinomial logistic regression[56]. Klang et al. [65] developed a prediction model using 595,561 ED visits to identify patients in the ED who require a head CT exam using a gradient boosting technique. The model was achieved an AUC of 0.93, with a specificity/sensitivity of 85.7%/88.1%.

AI in robotics has greatly influenced the healthcare industry, we can see that even though AI controlled robotic systems are used proficiently in healthcare laboratories and for manufacturing healthcare equipment with precision [152], it's adoption into mainstream medical practices like surgery has been scarce. Minimally invasive surgery is a great alternative to open surgery options as it reduces surgical trauma and eases post-surgery rehabilitation, but it comes with its own set of disadvantages as surgeons now need to handle a confined work space, with a reduced ability to judge distances and a decreased ability to coordinate the movement of their hands with their visual perception. There has been console operated robotic systems, like the da Vinci surgical system who is able to execute minimally invasive surgery by replication the hand movements of a surgeon with high precision. [45]. Concentric Tube Robots (CTRs) which are robots that have unlimited or indefinite degrees of freedom and joints. [119] has shown great potential for minimally invasive surgery due to its miniaturization potential and maneuverability [4].

The advent of AI in healthcare has also come as a boon for hospitals themselves. In the context of hospitals, re-admission typically refers to the situation where a patient is readmitted to the hospital within a specified period of time, often within 30 days of their initial admission. Ajay et al. [2] showed the cons of re-admission in hospitals and proposed how it can be prevented using ML techniques. Vivanco et al. [141] used ML techniques to identify patients likely to overstay in hospitals, these patients are partly responsible for high waiting times and bed shortages in the hospital.For patients at a tertiary teaching hospital, they were able to get an F-Measure of 0.826 using a decision tree classifier, whereas at a community hospital, they achieved an F-Measure of 0.784. Yala et al. [155] built a classifier to parse classical breast pathology reports automatically by extracting pertinent tumor characteristics into readily available data with an average accuracy of 97% of individual categories.

Hypoxaemia is the condition where there is an unusually low blood oxygen levels. Researchers were able to use a ML based system to predict the prevention of hypoxaemia during surgery. They were effectively able to double the rate of prediction of hypoxaemia by anesthesiologists from 15% originally to 30% with the use of their system [77]. Wijnberge et al. [153] used a ML algorithm that predicts hypotension during the time of surgery while taking into account personalized treatment. Hatib et al. [52] built a custom ML based algorithm to predict hypotension during the surgery, they were able to achieve a specificity of 87% and sensitivity of 88% 15 min in advance of a hypotensive event with an AUC of 0.95.

2.5 AI in COVID-19

Coronavirus Disease 2019 (COVID-19) is an infectious disease caused by Severe Acute Respiratory Syndrome Coronavirus 2 (SARS-CoV-2) Virus. The outbreak of COVID-19 rapidly spread across the world, bringing the global population to a standstill. Severe cases of COVID-19 may result in serious respiratory disease which might even lead to death. By the end of October 2021, WHO has confirmed over 4.9 million deaths due to COVID-19. AI interventions helped in controlling the pandemic. AI models were used to quickly and accurately identify individuals who are not wearing face masks [72, 13]. COVID-19 is a fast spreading infectious disease and can pose immense pressure on the existing health infrastructure of the world. Early prediction of an upcoming surge in the COVID-19 positive cases can help the authorities in taking proactive measures that can save thousands of lives. Researchers have developed AI based models for epidemic waves forecasting [149, 10, 97]. These models can predict the approximate time and intensity of the forthcoming surge of positive cases. Several prognostic and diagnostic applications of AI for COVID-19 are also being developed, proving the immense significance of AI in this fight.

2.5.1 AI based COVID-19 Diagnosis

It is crucial to find COVID-19 early in its life cycle in order to inhibit the virus's proliferation. Several studies tried to use AI based solutions to help in accurate and fast COVID-19 diagnosis. Many studies trained ML models using chest X-rays [12, 146, 102], while others tried to exploit the chest CT imaging [16, 60] for the diagnosis of COVID-19. Although radiological imaging based solutions tend to perform well, they are expensive and complex. Some studies proposed using cough or respiratory sound recordings for COVID-19 detection [90, 82, 91]. Aly et al [9] used a dataset of 1299 sound samples to train an ML model that detected COVID-19 positive samples with an AUC of 0.96. Zoabi et al [164] proposed an ML model trained on records of 51,831 individuals. The model could detect COVID-19 positive cases precisely by just using the symptoms and basic patient information like age and sex.

2.5.2 AI based COVID-19 Prognosis

COVID-19 had posed an unprecedented pressure on global health infrastructure due to the enormous inflow of patients demanding medical care. In times of distress, efficient utilisation of critical resources like oxygen and ventilators becomes an important step, which, if not appropriately enacted, can lead to the deaths of many. Early detection of people at high risk can be aided by the effective prognosis of COVID-19 patients. Authorities can then provide preferred medical care to individuals who stand a chance of developing severe complications, which might help in saving thousands of lives. Many AI solutions for early and quick COVID-19 prognosis were developed. Wang et al. [147] developed ML models exploiting laboratory and clinical features for COVID-19 mortality prediction. The models achieved an AUC of 0.83. Bolourani et al. [21] developed an ML model that utilised features like age, respiratory rate, serum lactate to predict respiratory failure with an accuracy of 91.9%. Additionally, ML models using chest CT and X-rays to forecast patient mortality and severity have been proposed. [31, 80].

2.6 Summary and Outlook

Although AI in Healthcare has shown excellent prospects, it faces many challenges. ML models are data-hungry systems that require enormous amounts of data for training. Healthcare data collection is an arduous task, and often healthcare datasets are inadequate and biased. Data scarcity poses a significant challenge to the success of AI in healthcare. Developing an AI for healthcare solution that generalises well is another challenging task. Often, inadequate and biased training data fails to represent the proper and complete subsample of the data. Healthcare datasets are often plagued with ethnic and racial biases, which pose a severe challenge in the generalizability of the ML and DL models. It is often seen that models trained on the data of the population of one subcontinent fail when tested on data from some other cohort. Under representation of the minority class in the dataset can lead to biased AI models that overfit the majority class. This bias can lead to the seclusion of minorities from the general medical practice. Data privacy is another big hurdle in the success of AI in healthcare. Lack of proper protocols to maintain the anonymity and privacy of intimate health information dissuades patients and hospitals from sharing the data with the researchers. Another big challenge is the lack of interpretability in the developed AI solutions. Many of the current ML and DL models utilized in healthcare are considered "black boxes" that provide a quantitative output without explaining the reasoning behind their decisions. This lack of interpretability and generalizability has led to a lack of trust in AI within the medical community. The healthcare industry has been hesitant to implement and expand AI solutions due to these concerns, resulting in friction in the growth of AI in healthcare at the operational level.

Even though many challenges loom ahead of the success of AI in healthcare, we believe in the coming future, AI will play a pivotal role in revolutionising the healthcare industry for good. Cumulative efforts of academia, industry and government authorities might help in the generation of more extensive and unbiased healthcare datasets. Development and training of the AI models which are uninhibited from racial and ethnic biases will be crucial in the success of AI in healthcare. Proper protocols and regulations need to be established to dismiss the concerns regarding data privacy and security. Developing trust toward the AI solution is also an essential attribute in the widescale adoption of AI in healthcare. We believe AI would not eliminate the need for human intervention; instead, it will assist radiologists and clinicians in providing more reliable, cheaper and easily accessible medical care to all.

Chapter 3

Single-Lead to Multi-Lead Electrocardiogram Reconstruction Using a Modified Attention U-Net Framework

3.1 Introduction and related works

An ECG is a non-invasive medical procedure used for heart activity monitoring. This procedure is widely used owing to its speed and effectiveness in detecting heart-related problems [78, 124]. An ECG can record heart's electrical activity using electrodes which are placed on the patient's skin, giving us information about the heart rhythm and health. These electrodes are conductive and are able to record the voltage present on the skin, which is then processed before being presented to the clinician for further diagnosis.

There are multiple variations of ECGs depending on the number of leads used, but the 12-lead ECG is widely considered the most commonly used in healthcare centers worldwide [105]. Even though it is called a 12-lead ECG, it only involves ten electrodes comprising four limb electrodes (placed on all four limbs of the patient) and six pre-cordial electrodes. An apparent problem with this type of ECG is the precision needed in placing the electrodes at suitable locations [101]. As clinicians are dependent on the collected signals to make a diagnosis, a small error in their placement can result in the production of unwanted artefacts in the signals, leading to a possibility of an erroneous diagnosis. Knight et al. [66] showed that 38% of 500 electrophysiologists who participated in their study misdiagnosed an artefact as ventricular tachycardia. Even though other variations of ECGs that need lesser leads do exist, they are relatively inaccurate compared to the 12-lead variant. This becomes a major hassle for patients who need continuous monitoring, where they are forced to sacrifice the accuracy of a 12-lead ECG for the portability and ease of use of lesser lead variants.

Although the 12-lead ECG only requires 10 electrodes, the 12 leads in the name stands for the processed signals obtained from these electrodes. The 12 generated leads can be divided into frontal plane limb leads (I, II, III, aVF, aVL and aVR) and chest leads (V1, V2, V3, V4, V5 and V6). The lead I is calculated by substracting the left and right arm electrodes. The lead II is calculated by sustracting the left leg and right arm electrodes. The lead III is calculated by sustracting the left arm and left leg electrodes. The remaining three frontal plane limbs are called the augmented vector (aV) leads, where the F, L and R in their names represent the Foot, Left arm and Right Arm, respectively. These leads are mathematically derived from the first three limb leads. Using Kirchoff's law on electrical current, which states the sum of all currents in a closed circuit is zero [79], we can mathematically generate all frontal plane limb leads using any two of the frontal plane limb lead values. The chest leads are not interrelated like the frontal plane limb leads and hence have to be recorded individually using separate electrodes (V1 to V6). The electrode on the right leg is not used to generate any lead; instead, it is used as ground to prevent artefacts in the other leads. [43]

Due to various intricacies involved, the usage of the 12-lead ECG is restricted in pre-hospital, ambulatory and home-care settings. With cardiac-related issues becoming more prominent around the world [61], accurate but easy-to-use ECG devices are needed more than ever. Even though devices like the Holter monitor [30] exist, which measure the standard 12-lead ECG, their utility is limited by the movement constraints they put on their user. With recent technological advances, we have witnessed much growth in the wearable technology field, from smartwatches used by the masses to more sophisticated straps used by athletes. The major drawback with such devices is that they almost always only collect a subset of the twelve leads. Even though this information is helpful, a clinician is usually trained to interpret a 12-lead ECG, thus handicapping the utility of such devices. ECG reconstruction can help bridge this gap by converting reduced lead set ECG to standard, more interpretable 12-lead ECG. One should note that ECG reconstruction does not add new information to reduced lead set data. Instead, it just converts all the information captured in the reduced lead data into a 12-lead version. As the human heart-torso electrical system is theoretically linear and quasi-stationary, the initial reconstruction efforts using ML techniques were limited to the use of Linear Regressors [17, 51]. However, as computational capabilities have improved in recent times, researchers found eminent success in synthesising more accurate signals using neural networks.

Several studies [162, 148, 59, 120] have achieved good reconstruction results from a reduced lead set. Huaiyu et al. [162] presented a synthesis algorithm called ARSPL, which stands for adaptive region segmentation-based piece-wise linear algorithm, that can reconstruct standard 12-lead electrocardiogram (ECG) signals using only a 3-lead subset (specifically, leads I, II, and V2). They first detected R-peaks in the signal before performing segmentation; each segment is further divided into cardiac electrical activity stages. Each sub-segment is then fed to different Linear Regressors for final ECG generation. They achieved an average pearson correlation of 0.947 and an average RMSE of $55.4\mu V$ on the generated leads. Wang et al. [148] presented a novel method to generate all 12 leads using just a 3-lead subset (I, II and V2) using convolutional neural networks. They convert the 1-D ECG signal into 2-D images using slipping conversion before passing it through multiple convolutional layers. Their methods are able to beat both multiple regression-based methods and artificial neural networks committees-based methods in most of the generated leads. Using a custom-designed piece of hardware acting as a three-lead patch-type ECG device and employing a long short-term memory network, Jangjay et al. [120] achieved an average correlation coefficient of 0.95 for their reconstructed signals.

According to the authors, by utilizing LSTMs, they can address the problem of reduced horizontal vector components in the electric signal captured using their own device. The authors further validate their improvements by showing the ability to detect pathological abnormalities with comparable accuracy to the 12 lead ECG. Kapfo et al. [59] propose a method that is tailored to individual patients for reconstructing the standard 12-lead ECG. They also use a discrete wavelet transform (DWT) combined with LSTMs to predict the standard 12 leads using just three input leads. They achieve an average correlation constant of 0.98 and a RMSE score of 78. However, all the mentioned studies were dependent on three different leads (two frontal limb leads and one pre-cordial lead). This hinders their practical use, as they would still require multiple electrodes to be placed on the chest and multiple limbs to collect the required signal. To fast-track the adoption of such reconstruction techniques by the wearable device industry, we need to reduce the amount of data they need to collect.

Gundlapalle et al. [49] introduced a novel method for reconstructing a 12-lead ECG using a single lead input, using CNNs, LSTM units, and multi-layer perceptrons. With only lead II as input, they generated the other 11 leads, achieving an average correlation of 0.973 and a regression coefficient of 0.959. Yoon et al. [156] developed a generative adversarial network (GAN) to generate all 12 leads of an ECG using a single lead (lead I) as input. They utilized a U-net as their generator and a patch discriminator as their discriminator. Their model was able to reconstruct signals with a mean Frechet distance (FD) score of 11.321 and a mean square error of 0.038.

To the best of our knowledge, these were the only studies performing ECG lead reconstruction using a single lead. Both these works suffer from some critical drawbacks. Both works segment their signals to shorter lengths (1 second and 2.5 seconds) while generating the other leads for relatively easier reconstruction. However, as traditionally, ECG is recorded for 10 seconds [24], to use the proposed approaches in real life, one would need to develop algorithms to connect the reconstructed segments together, which might reduce the effectiveness of the overall reconstruction. Both works use a complex set of deep-learning algorithms. Yoon et al. [156] used a GAN, which is hampered by unstable learning and takes a very long time to train [154]. Gunlapelle et al. used a combination of CNNs, LSTMs and MLPs, making the overall pipeline very complex. Gunlapelle et al. also segmented the ECG signals into 1-second segments, which were then randomly divided into train and test sets. This could have caused 1-second ECG segments belonging to the same ECG signal to be present in the train and the test set. This leakage of data might have inflated the reported results. Although both studies produced good signal reconstruction, they did not establish whether the reconstructed signals can be used in real-life applications.

In this study, we present a Modified Attention U-Net based framework for Single-Lead to Multi-Lead Electrocardiogram Reconstruction. We used the lead II to reconstruct the remaining 11 leads with a mean Pearson Correlation coefficient of 0.805. Since only lead II is used as an input, the desired data can easily be calculated using just two electrodes placed on the left leg and right arm. We improve on the drawbacks of previous works and also demonstrate that the reconstructed ECG signal can be used by a classification model trained on a standard 12-lead ECG data to detect cardiovascular diseases efficiently. Our contributions are:

- Instead of using shorter ECG segments for reconstruction, we reconstruct the complete 10-second ECG signal at once.
- We propose a model architecture which only employs convolutions, making them easily malleable to work with any size input segments while training is faster.
- We propose a modified variant of Attention U-Net performing better than the standard U-Net and Attention U-Net.
- Unlike the past studies, which use a separate model for each lead reconstruction leading to a total of 11 models, we use a single model for all 11 lead reconstructions. By using a single model, not only were we able to reduce the number of trainable parameters but also were able to improve upon the performance.
- We test our reconstructed signals on an existing 12-lead disease classification model to accurately measure how well our method can preserve anomalies in the input signal that the classification model uses for disease detection.

3.2 Methods

3.2.1 Dataset and preprocessing

For the study, we used the large publicly available PTBXL dataset [143]. The dataset has 21837, 10-second length, 12-lead ECG data from 18885 patients collected over a period of seven years. The ECG signals are provided with sampling rates of 100Hz and 500Hz. For this study, we employed ECG signals sampled at 500Hz. The dataset includes a large portion of healthy records as well as a wide range of diagnostic classes like myocardial infarction, hypertrophy, etc. As part of the data preprocessing, we first used a Butterworth [34, 46] highpass filter set at 0.5Hz to remove the low-frequency noise and artefacts. This was followed by a Butterworth lowpass filter set at 200Hz to remove the high-frequency noise. Finally, all the ECG signals were smoothed using Savitzky-Golay Filter[111].The dataset was divided into training and testing sets using an 80%-20% split, where 80% of the data was used for training and 20% for testing. The training set contained 17469 ECG recordings, while the testing set contained 4368 ECG recordings.

3.2.2 Model Architecture

Fig. 3.1 represents the proposed Deep Learning architecture we use for lead reconstruction. We propose a single model which takes the lead II of the original ECG as input to reconstruct the remaining

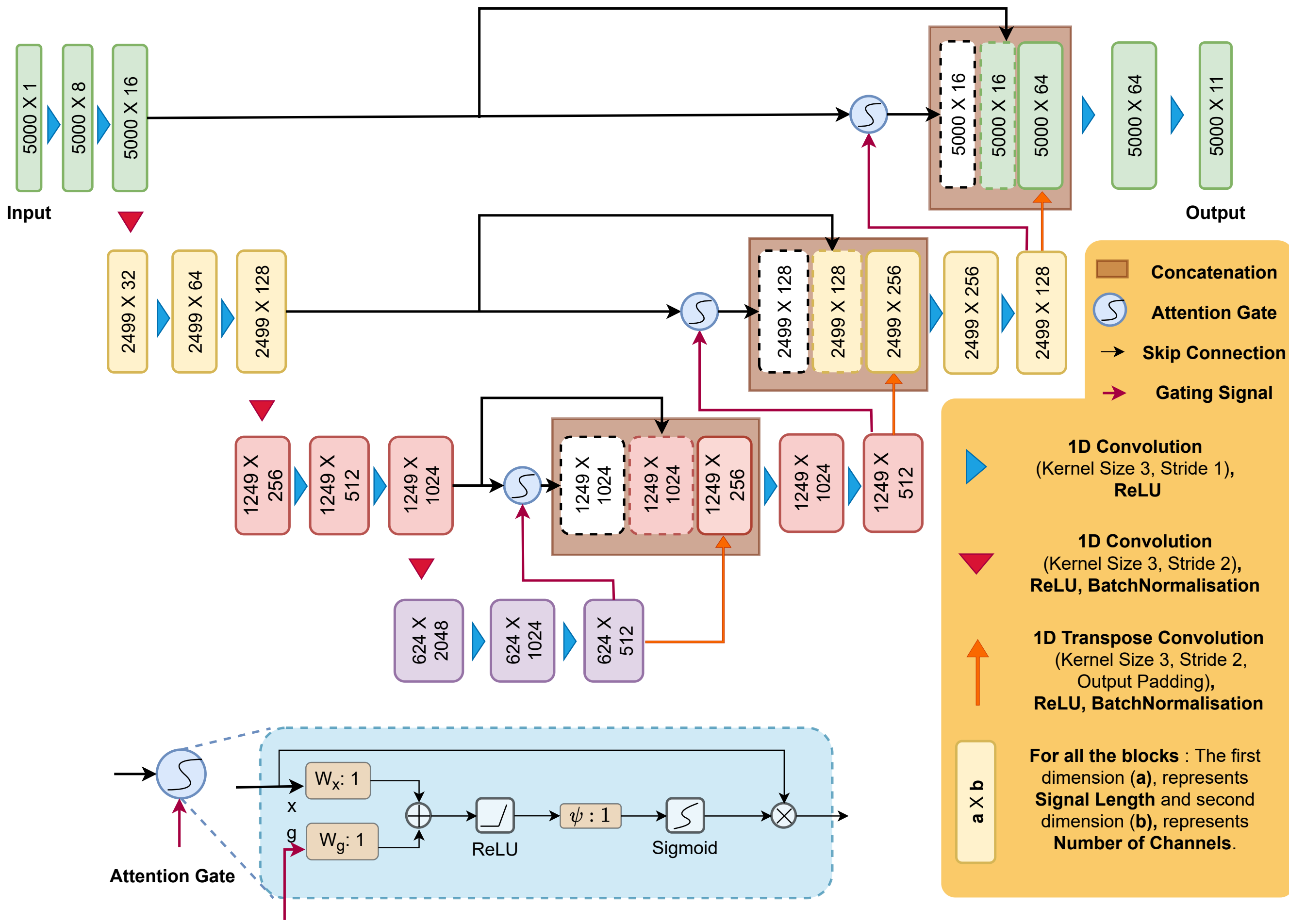

Figure 3.1: Model Architecture of the proposed model.

11 leads. Since both input and output data are time series signals, we use 1D convolutions to design the network. The input is a single channel 5000-length signal representing a 10-second recording of the lead II sampled at 500Hz. The output comprises 11 channels of 5000 in length, where each channel represents the different leads of the reconstructed ECG signal.

The model architecture used in the study is a modified version of the Attention U-Net proposed by Oktay et al. [88]. A U-Net architecture first downscales the input and then upscales the downscaled input back to generate the output. The skip connections are employed to tackle any data loss. In the proposed model architecture, we downscale the input lead II signal thrice, which is then upscaled thrice to get the reconstructed leads. Standard attention U-Net employs max-pooling for downscaling the signals while upsampling layer is used for upscaling. The convolution layer provides a kernel with learnable parameters, which the max-pooling layer lacks; hence we replace the max-pooling in the original attention U-Net with a 1D convolution of stride 2 and kernel size 3. Similarly, the upsampling layer is replaced by a 1D Transpose Convolution [39] of stride 2 and kernel size 3. The standard attention U-Net applies attention to the skip connection to get the attention-gated skip connection. This attention-gated skip connection is then used for concatenation with the upscaled signal from the 1D Transpose Convolution. For the proposed model, we concatenate the raw skip connection in addition to the attention-gated skip connection with the upscaled signal.

3.2.3 Model Training and Testing

The proposed model is trained on the training set for 50 Epochs. The ADAM optimiser is used for optimisation [64] and Mean Squared Error is used as the target loss function. The Batch Size was set at 32 for training. The learning rate was initially set at 0.0001, which was reduced on plateauing of the loss using a scheduler. The trained model was then tested on the hold-out test set, and different evaluation metrics were used to evaluate the quality of signal reconstruction. The model was trained and evaluated using NVIDIA GeForce GTX 3090Ti with 24 GB memory. Pytorch version '1.12.1' [96] was used for the realisation of the model. Similar training and testing regimes were followed for all the other models mentioned in the Results and Experiments Section.

3.2.4 Evaluation Metrics

To evaluate the quality of ECG reconstruction, we used the three metrics.

- The Pearson Correlation coefficient(ρ) represents the similarity between the reconstructed and the original signal. ρ ranges from -1 to 1, where 1 represents that the two signals are exactly the same, while -1 represents that the two signals are exactly opposite.

$$\rho = \frac{\sum_{i=1}^{n}(x_i - \bar{x})(y_i - \bar{y})}{\sqrt{\sum_{i=1}^{n}(x_i - \bar{x})^2 \sum_{i=1}^{n}(y_i - \bar{y})^2}} \tag{3.1}$$

- The Mean squared error (MSE) measures the average error between the generated and the original signal. Thus the lower the MSE, the better the signal reconstruction, and an MSE of 0 will represent that the reconstructed signal is exactly identical to the original signal.

$$MSE = \frac{1}{n}\sum_{i=1}^{n}(x_i - y_i)^2 \tag{3.2}$$

- The level of association between the original and generated signals has been assessed using R^2 statistics. The R^2 value of a perfectly reconstructed signal will be 1.

$$R^2 = 1 - \frac{\sum_{i=1}^{n}(x_i - y_i)^2}{\sum_{i=1}^{n}(x_i - \bar{x})^2} \tag{3.3}$$

  Where x_i is the i$^{\text{th}}$ data point of the original signal and y_i is the i$^{\text{th}}$ datapoint of the reconstructed signal. $\bar{x}$ and $\bar{y}$ are the sample means of the original and reconstructed signal respectively, and n is the number of data points in the signal.

3.3 Experiments and Results

3.3.1 Performance Analysis and Comparison

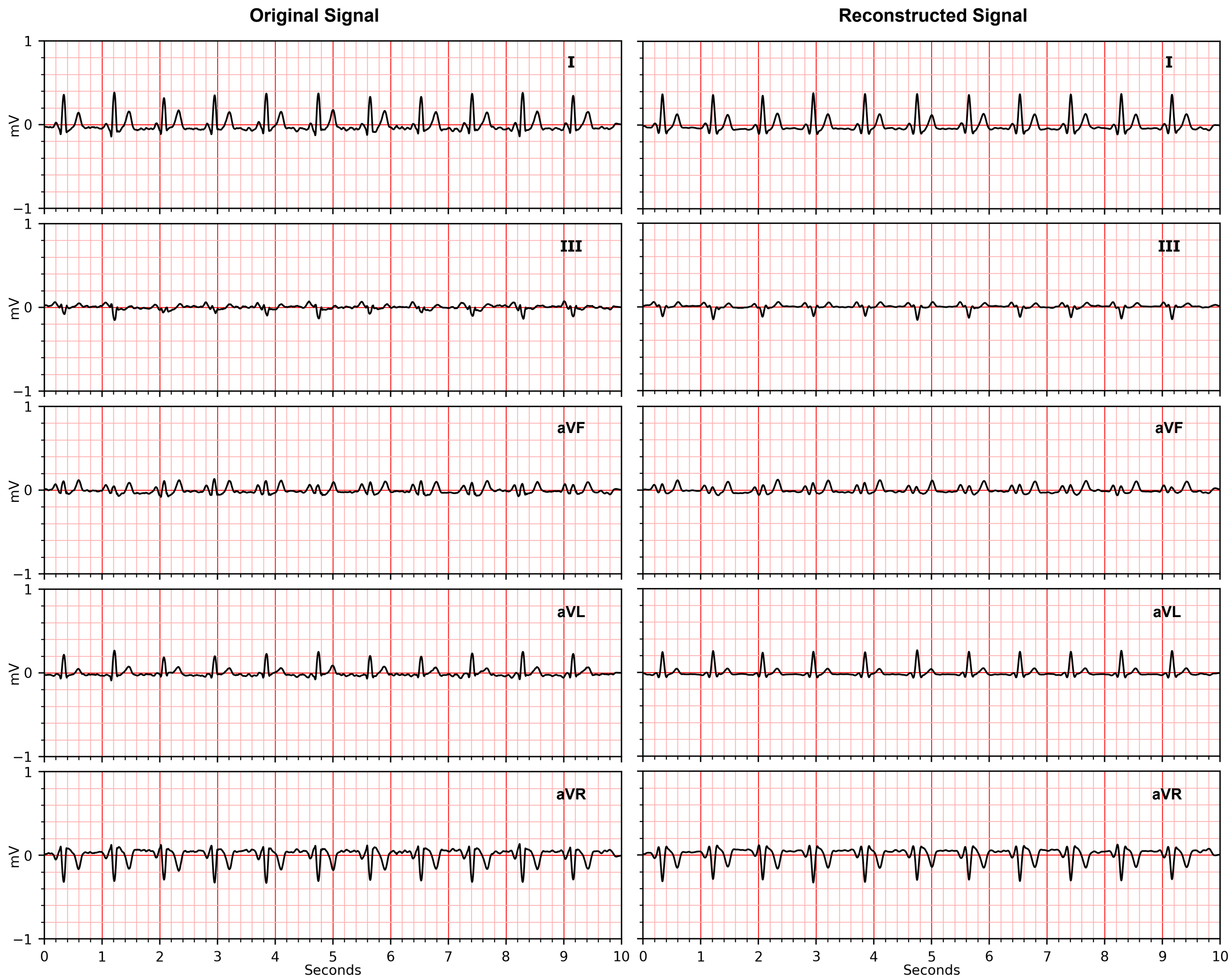

Figure 3.2: The original and the reconstructed signals for the frontal plane limb leads I, III, aVF, aVL and aVR using the proposed model.

The proposed model reconstructed the 11 leads from lead II with a mean Pearson Correlation coefficient (ρ) of 0.805, MSE of 0.0122, R^2 of 0.639. We compared the results of the proposed model with those of other models, and the results are summarized in Table 3.1.

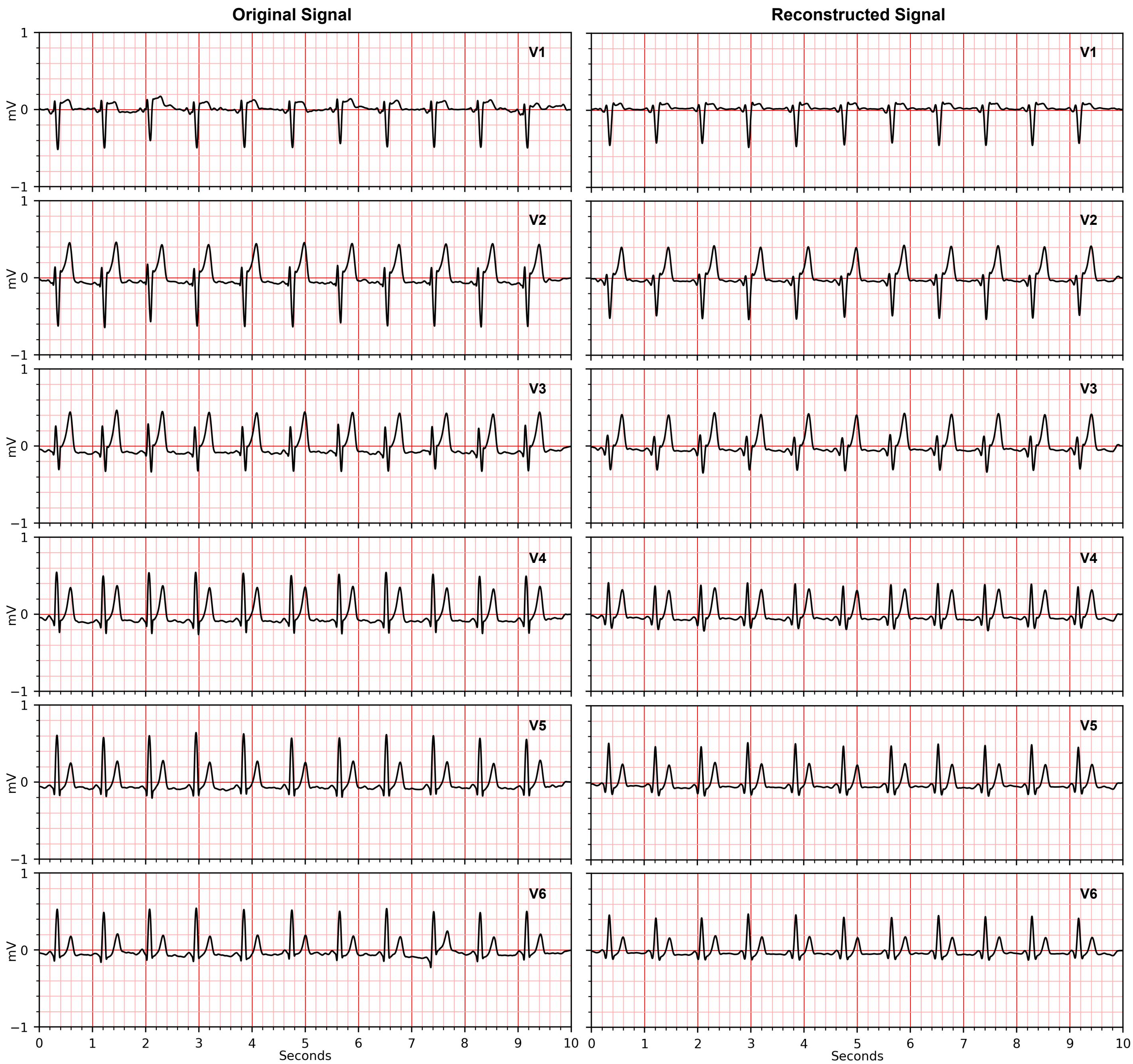

Figure 3.3: The original and the reconstructed signals for the chest leads V1, V2, V3, V4, V5, V6 using the proposed model.

A standard U-Net with 3 downscaling and upscaling layers similar to the proposed model gave a mean Pearson Correlation Coefficient of 0.750. Given that 1D Convolutions have learnable parameters, we replaced the Max-Pool layer in the standard U-Net with a 1D Convolution with stride 2 and Kernel

Model	ρ	MSE	R^2
U-Net	0.750	0.0159	0.528
Modified U-Net	0.784	0.0138	0.591
Modified U-Net with Attention	0.790	0.0132	0.610
Proposed Model	**0.805**	**0.0122**	**0.639**

Table 3.1: Performance Analysis of the proposed model for lead II to 12-lead reconstruction task. All model improvements were statistically significant with p-values $\ll 0.05$.

size 3. Similarly, the Upsampling layer was replaced with a 1D Transpose Convolution of kernel size 3 and stride 2. We can refer to this model as a modified U-Net. This modified U-Net improved upon the conventional U-Net with a mean Pearson correlation coefficient score of 0.784. The improvement of results validates the use of 1D Convolutions and 1D Transpose Convolutions over max-pooling and upsampling. Attention can further help in better localization and can help the model understand which part of the input needs to be focused upon [15]. Thus adding attention to the skip connection could help the network to localise to the area of importance in the skip connection. An attention block inspired by Oktay et al. [88] was added to the skip connection of the modified U-Net where the max-pooling layer was already changed with the 1D Convolution layer, and the upsampling layer was changed with the 1D Transpose Convolution. We can refer to this model as Modified U-Net with Attention. This model further improved the results to a mean Pearson Correlation coefficient of 0.790. Thus attention helped the model better understand the lead reconstruction task. This modified U-Net with attention just like the standard attention U-Net used the attention to the skip connection. Then the attention-gated skip connections are concatenated with the upscaled signal coming from the 1D Transpose Convolution. For the proposed model, we experimented by concatenating the raw skip connection in addition to the attention-gated skip connection with the upscaled signal. The proposed model gave the best metrics with a mean Pearson Correlation coefficient of 0.805. We also tested the GAN architecture similar to the one proposed by Yoon et al. [156] but modified to work with the 10-second length ECG signal. Although the GAN took significantly longer to train, the results produced were not able to beat the proposed model. We can inspect the quality of ECG reconstruction for the frontal plane limb leads using Fig. 3.2, and Fig. 3.3 can be used to examine the reconstruction of the chest leads.

3.3.2 Comparison between Single-to-Multi lead model & Single-to-Single lead Model

Yoon et al. [156], and Gundlapalle et al. [49] both used 11 deep learning models, each responsible for converting the original lead to a single lead. We compared the results between the single-to-multi lead model, where a single model is responsible for converting the lead II to the 11 other leads to that of single-to-single lead models, where each model is responsible for converting the lead II to one of the 11 other leads. We used the model architecture defined in the Methods section for the single-to-multi lead model. For the single-to-single lead model, we changed the last layer of the proposed model so that instead of outputting 11 channels; the model has a single-channel output. Both the models were trained and tested using the regime explained in the Methods section. Table 3.2 provides the results for each lead conversion for the single-to-single lead and single-to-multi lead models. We can observe that the single-to-multi lead model performed better for the signal reconstruction for all 11 leads compared to the single-to-single lead models with respect to all three evaluation metrics. The single-to-multi lead model might be performing better owing to its ability to employ the backpropagating gradients from all 11 leads and combine them to get a better latent space representation of the lead II. The single-to-single lead model only has information concerning a single lead it is trying to reconstruct; thus, the latent space representation for the model might be inferior to that of the single-to-multi lead model.

Lead	Single-to-Single lead			Single-to-Multi lead		
	ρ	MSE	R^2	ρ	MSE	R^2
I	0.841	0.0053	0.610	**0.847**	**0.0049**	**0.633**
III	0.657	0.0055	0.611	**0.663**	**0.0047**	**0.658**
aVL	0.616	0.0052	0.491	**0.659**	**0.0047**	**0.536**
aVR	0.934	0.0015	0.850	**0.935**	**0.0015**	**0.853**
aVF	0.883	0.0015	0.855	**0.892**	**0.0013**	**0.873**
V1	0.811	0.0135	0.539	**0.818**	**0.0113**	**0.611**
V2	0.767	0.0349	0.507	**0.778**	**0.0317**	**0.552**
V3	0.722	0.0360	0.428	**0.728**	**0.0333**	**0.470**
V4	0.772	0.0234	0.473	**0.785**	**0.0222**	**0.499**
V5	0.857	0.0120	0.640	**0.859**	**0.0120**	**0.641**
V6	0.884	0.0076	0.678	**0.888**	**0.0071**	**0.698**

Table 3.2: Performance comparison of the single-to-single lead models with the single-to-multi lead model for lead II to 12-lead ECG reconstruction task. For all the leads except aVR the p-value was $\ll$0.05, suggesting statistical significance of the results. The p-value for aVR lead was 0.191.

3.3.3 Cardiovascular Disease Classification

In our previous experiments, our concern has always been how well the model performs for the chosen evaluation metrics. However, we realized that the main aim of performing lead reconstruction should be making sure that the final generated signals are usable in real-world scenarios by clinicians, classification models, etc. That is, these generated signals should be able to act as a replacement for standard 12-lead ECG without any other intervention. From this perspective, even though evaluation metrics can tell us how well the signals as a whole have been reconstructed, they cannot tell us if essential artefacts in the signals used by clinicians for diagnosis and machine learning pipelines for classification have been conserved. There are chances where the signal has been reconstructed well, as all the rhythmic heartbeats have been preserved. However, the signal might still lack the artefacts needed by a clinician to diagnose the patient, rendering such a reconstruction useless. All previous works in the field have only focused on evaluating the signal quality quantitatively, making it unclear if the generated signals from these works can be used as 12-lead ECG replacements. We employed this experiment to verify if our model can generate signals conserving critical artefacts needed for diagnosis.

Ribeiro et al. [104] used an ensemble of neural networks with a Residual Network based architecture for 12-lead ECG multi-classification. They use a superset of the PTB-XL dataset, containing six databases from four different countries (United States, Russia, Germany and China) to build an end-to-end pipeline capable of classifying 12-lead ECGs according to 27 different classes. Using this work as our baseline, we utilized a single model from their ensemble as the classification model for our experiment. This classification model is a combination of a one-dimensional Residual Network containing five residual blocks and a final fully connected layer. The model was trained on all default parameters set by the authors in the original papers for 70 epochs. To ensure that our results are robust, we trained this classification model on the same training data used for training the ECG reconstruction model. We also test the model on the same test data on which the reconstruction models were evaluated. This ensures that no signals used to train the reconstruction model are used to assess the performance of the classification model. Thus, the test set is completely blind for both the reconstruction and classification models, mimicking a real-world use case. This classification model is now trained on the training set of the preprocessed PTB-XL data discussed in the Methods section, and the trained model is used for further evaluation. We test this trained model with two different approaches. First, the model was evaluated on the test set, where all 12 leads were the original leads provided in the dataset. The results can thus be used as a baseline for the following approach. We will refer to this approach as the Original Signals approach in the coming parts of the paper. In the second approach, instead of testing the classification model on the original signals, we tested it on reconstructed signals. We trained the lead reconstruction model on the training set to convert lead II to the 11 other leads. This reconstruction model was then used to reconstruct the 12-lead ECG from the lead II signals of the test set. This set of original lead II and reconstructed 11 leads were then given as input to the classification model. We must note that for both approaches, the classification model was trained on the training set where all 12 leads were the original signals, just that the testing regimes were different. Thus, the classification model was never trained on a reconstructed ECG signal. We will refer to the second approach as the Reconstructed Signals approach. We can observe the results of the two approaches using Table 3.3.

Model	AUROC	Accuracy
Original signals	0.810	0.456
Reconstructed Signals	0.752	0.426

Table 3.3: Performance comparison of cardiovascular disease detection for the original and reconstructed signals.

We obtained an accuracy of 45.6% and AUC of 0.810 for the original signals approach, and we obtained an accuracy of 42.6% and an AUC of 0.752 on the reconstructed data. We need to notice that this being a multi-class classification task with 27 classes, the chance accuracy would be close to zero. The drop in performance for the reconstructed signals approach was expected as the data of 11 leads has been eliminated entirely. However, the performance of the classification model using the reconstructed signal approach is comparable to the original signals approach. We can thus infer that our reconstruction model is able to preserve the necessary artefacts needed for classification from the original lead and reproduce it in all the reconstructed leads. This experiment shows that our reconstruction model is able to use data from a single lead and present it in such a way that a classification model trained to classify only based on 12-lead ECG is still able to work comparably.

3.4 Discussions and conclusions

ECGs play a major role in cardiovascular diagnostic decisions. With the rise in technology and increased awareness of health metric tracking, we are witnessing significant innovations in the wearable device sector using ECG signals. A considerable hurdle such device-makers face is that the wearables collect a reduced lead set of the ECG. Existing solutions in the automatic ECG classification space are built using the standard 12-Lead ECG as inputs, thus rendering the ECG unusable when only a subset of leads are collected. Likewise, in medical settings too, clinicians trained to diagnose based on a 12-lead ECG may find it challenging to interpret a reduced lead set data. ECG reconstruction primarily tries to bridge this gap between the influx of reduced lead set data from modern wearable devices and the consumption of standardised 12-Lead ECG data by clinicians and ECG analysis models. It is important to note that ECG reconstruction cannot add new information to reduced lead set data to create new 12-lead data. Instead, it rather converts all the information captured in the reduced lead data into a more interpretable 12-lead version.

In this work, we present a novel end-to-end Single-Lead to Multi-Lead Electrocardiogram Reconstruction pipeline. We use a modified attention-based U-Net model on the publicly available PTB-XL dataset to develop a method capable of using a single lead II to generate all other 11 leads of a standard 12-Lead ECG. We achieved a Pearson Correlation, Mean Square Error and R-squared value of 0.805, 0.0122 and 0.639, respectively. A significant drawback with the current ECG reconstruction studies is that they use three leads to reconstruct the 12-lead ECG signal. However, the current work overcomes significant limitations of earlier studies. Both previous studies divide the standard 10-second ECG signal into smaller segments for reconstruction. Generally, ECGs are recorded for 10 seconds; thus, one will be forced to use various algorithms to join the reconstructed segments, leaving their final performance questionable. Keeping this in mind, we developed our method to take a complete 10 seconds signal from lead II as input and reconstruct them into a 12-lead ECG of 10 seconds. Compared to past studies, we also use a relatively simple model comprising only convolutional layers making the whole network much easier to train; also, the same network can be employed to process other lengths of ECGs as input. Instead of using multiple models for generating all leads separately like in previous works, we use a single combined model to generate all 11 leads together, reducing the total parameters needed for models to work and resulting in faster training times. Using a combined model also helped us improve performance, as observed in the above section. Looking through current works in ECG reconstruction, a very noticeable flaw in how the models are evaluated seems to exist. The metrics only seem to be representative of how well the reconstruction is but do not try to identify if the reconstructed signal can actually be used in real-life applications. Thus, we must ensure that a reconstructive model can capture the necessary artefacts from the input signal, which are essential for diagnostic uses. Therefore, we devised an experiment to see if the reconstructed signals can actually be used by existing models that use standard 12-lead ECG data to detect cardiovascular diseases. In the experiment, we train a multi-disease classifier based on existing literature on actual 12-lead ECG data and see the drop in performance when tested on reconstructed 12-lead data. We observe that the classification model's performance while using the reconstructed signals was comparable to its performance using the original signals. This shows that our reconstruction model is capable of preserving artefacts from the original data, which might prove vital for uses like diagnosis by clinicians and predictive models.

The limited availability of ECG and healthcare data more generally presents a significant obstacle to the widespread adoption of AI in healthcare. Current volumes of ECG data are insufficient to support data-intensive models like transformers, which tend to perform poorly with the available data. However, the increasing digitization of the healthcare industry is expected to produce a surge in data in the near future, rendering the use of models like transformers more feasible. Healthcare data often contain cohort-specific features that can make a model trained on one cohort useless when applied to another. To address this issue, a study employing a dataset collected from multiple cohorts for training and evaluating ECG reconstruction models might enhance the generalizability of such models, which is presently lacking in this study. Although collecting single-lead ECG data is comparatively easier than multi-lead ECG data, it still requires the placement of at least two electrodes, which can be a complicated process. As a result, the need for an even simpler method to collect heart monitoring data persists.

Chapter 4

PPG to Single-Lead ECG Conversion using Wasserstein Generative Adversarial Netwroks

4.1 Introduction and Related Works

With the growing incidence of cardiovascular diseases worldwide [86], the continuous monitoring of heart health has become crucial. The ECG is widely recognized as the gold standard for measuring cardiovascular activity and is a fundamental tool for diagnosing CVDs [78, 124]. As discussed in Chapter 3 measuring the 12-lead ECG signals is a challenging task that requires a trained medical practitioner. Despite being a relatively straightforward procedure, obtaining a single lead ECG still necessitates the placement of at least two electrodes and can be a technical process. As a result, there remains a pressing need for a simpler method of collecting heart monitoring data.

Photoplethysmography (PPG) is a non-invasive technique utilized to evaluate changes in blood volume in the microvascular bed of tissue [5]. By detecting changes in blood flow, PPG can provide heart activity data. PPG measures the amount of light absorbed or reflected by the tissue by illuminating a light on the skin. The amount of blood in the tissue, which varies with each heartbeat, affects how much light is absorbed or reflected, allowing the monitoring of heart rhythm and rate. PPG is a convenient diagnostic tool as it is a simple and quick test that can be performed in a doctor's office or patient's house without any special preparation or equipment.

Continuous monitoring of ECG is often hindered by movement constraints imposed by monitoring tools. In contrast, PPG is a simple and easily measurable technique that can be continuously monitored using wearable devices such as smartwatches. While PPG can be easily collected, the lack of adequate knowledge and techniques for analyzing it implies that ECG remains the gold standard for medical diagnosis, given the abundant scientific knowledge backing it up. The PPG and ECG readings are naturally interconnected as changes in peripheral blood volume are driven by left ventricular myocardial activity, which is regulated by electrical impulses arising from the sinoatrial node. The physiological features of PPG waveform like timing, amplitude, and shape reveal how the heart and connective tissue interact. The relationship between ECG and PPG signals can be utilized to develop a technique for reconstructing ECG signals from PPG signals. This approach can bridge the gap between the ease of PPG measurement and the technical expertise required for ECG analysis.

Although the task of ECG reconstruction from PPG is promising, the currently available literature is limited. Zhu et al. [163] were the first to portray the idea of generating ECG using PPG. The authors proposed a Discrete Cosine Transform (DCT) based solution to convert each PPG heart cycle to its corresponding ECG cycle. The DCT coefficients of each PPG cycle are mapped to the associated ECG cycle using a transform matrix which is identified using ridge regression. The authors were able to reconstruct ECG with a Pearson correlation of 0.954. To create the QRS Complex of the ECG using the associated PPG signal, Chiu et al. presented a deep learning architecture [28]. They proposed an encoder-decoder architecture comprised of a sequence transformer and attention network. The authors also proposed a new QRS enhanced loss to improve the training. The authors used the University of Queensland Datset (UQVSD) [70], comprising 32 patients whose PPG and ECG were recorded for 55 hours. The QRS complex was produced using the suggested technique with a normalised root mean squared error of 0.107. Li et al. [69] proposed a lightweight neural network for ECG generation and CVD detection using the PPG. The authors proposed an encoder-decoder architecture using the proposed feature extractor and feature transform modules proposed in the study. The authors also used an attention gate to connect the encoder and decoder in order to make up for the loss of high-resolution features. The authors used the Medical Information Mart for Intensive Care III (MIMIC-III) database [58] and were able to generate the ECG with a relative RMSE of 0.34.

The three studies mentioned above - Zhu et al. [163], Chiu et al. [28], and Li et al. [69] - had extensive data preprocessing pipelines. These preprocessing pipelines involved segmenting the PPG data such that only a single cycle of heartbeat is present in each segment. This segmented data was then used to regenerate the ECG heartbeat. However, generating the complete ECG signal from these segments is a challenging task as joining these segments together could lead to a decrease in the overall quality of the generated ECG. Segmenting signals into cycles is also a difficult task since the heart rate tends to vary, leading to different segment lengths because of the changing heart cycle lengths. Vo et al. [142] proposed a new approach to generate ECG from PPG using Generative Adversarial Network (GAN) [47]. Unlike the other studies, the authors did not employ complicated data preprocessing pipelines, making the model easier to implement in real-life scenarios. The proposed method also did not use cycle-wise segmentation; instead, it segmented the data into 3-second segments. This allowed the model to generate ECG with multiple heart cycles at once. The authors used a GAN with Wasserstein loss and gradient penalty [11, 48] for their proposed method. They used a U-Net [106] as the generator and a PatchGAN as the discriminator. They used the data of 276 randomly picked patients from the Multi-parameter Intelligent Monitoring in Intensive Care (MIMIC) II database for training and evaluation. The proposed method was able to generate the ECG with a Pearson correlation of 0.835, which is a promising result and shows the potential of this approach.

The studies discussed above have a limitation in their experimental design that could affect the validity of their results. This limitation is the insufficient patient-level splitting during data segmentation.

In these studies, patients were recorded for multiple hours of continuous PPG and ECG signals, which were then segmented into smaller segments and randomly assigned to the training or testing sets. The problem with this approach is that it may lead to inflated results since the model is tested on data from patients that it has already been trained on. This limitation undermines the credibility of the results of these studies. To overcome this limitation, our study has taken measures to ensure that the train and test set patients are distinct. This approach helps to validate the performance of the model in a real-world scenario. Furthermore, we have implemented an encoder-decoder network to independently encode and decode ECG and PPG signals into their respective latent space representations to explore the independent encoding and decoding of ECG and PPG signals. In addition, we have proposed a Wasserstein Generative Adversarial Network - Gradient Penalty (WGAN-GP) that employs a U-Net++ as a generator to generate lead II ECG signals using the underlying PPG signals. The model performed the best on the task of generating ECG from PPG when compared to other models.

4.2 Methods

4.2.1 Dataset and Preprocessing

The MIMIC II waveform database, a publicly available dataset of simultaneous ECG and PPG recordings from thousands of patients collected across multiple hospitals between 2001 and 2008, was used in this study. All signals in the dataset were sampled at 125 Hz, and the processed version of the dataset available online was used [44]. Due to the presence of a high amount of noise and artificial artifacts in the ECG and PPG signals in the MIMIC II dataset, bandpass filters were applied for denoising purposes [34, 46]. A highpass bandpass filter with a cutoff frequency of 0.05 Hz was used to remove low-frequency noise in the ECG signals, while a cutoff frequency of 0.5 Hz was used for the PPG signals. Similarly, a lowpass bandpass filter with a cutoff frequency of 50 Hz was applied to remove high-frequency noise in both ECG and PPG signals. The effect of bandpass filtering can be observed in Figure 4.1.

To ensure accurate analysis and comparison of electrocardiogram (ECG) and photoplethysmogram (PPG) signals, it is crucial to align them spatially. We employed a signal alignment technique to obtain spatially aligned ECG and PPG signal pairs, taking into account potential signal pair misalignment. First, we used SciPy [140] to detect the peaks of all the heart cycles of the PPG and R peaks in ECG signals. The detected PPG peaks and R peaks of ECG were then utilized for signal alignment. In cases where multiple peaks were detected within 1.5 or lesser heart cycles, or if a peak was detected for only one of the ECG or PPG signals and not for the other signal within half a heartbeat, those peaks were removed from further analysis to ensure accuracy. The final cleaned sets of ECG and PPG peaks were then used to identify the signal misalignment. The effectiveness of our signal alignment approach is demonstrated in Figure 4.2, where misaligned ECG and PPG signals for two random patients in the dataset are aligned for comparison.

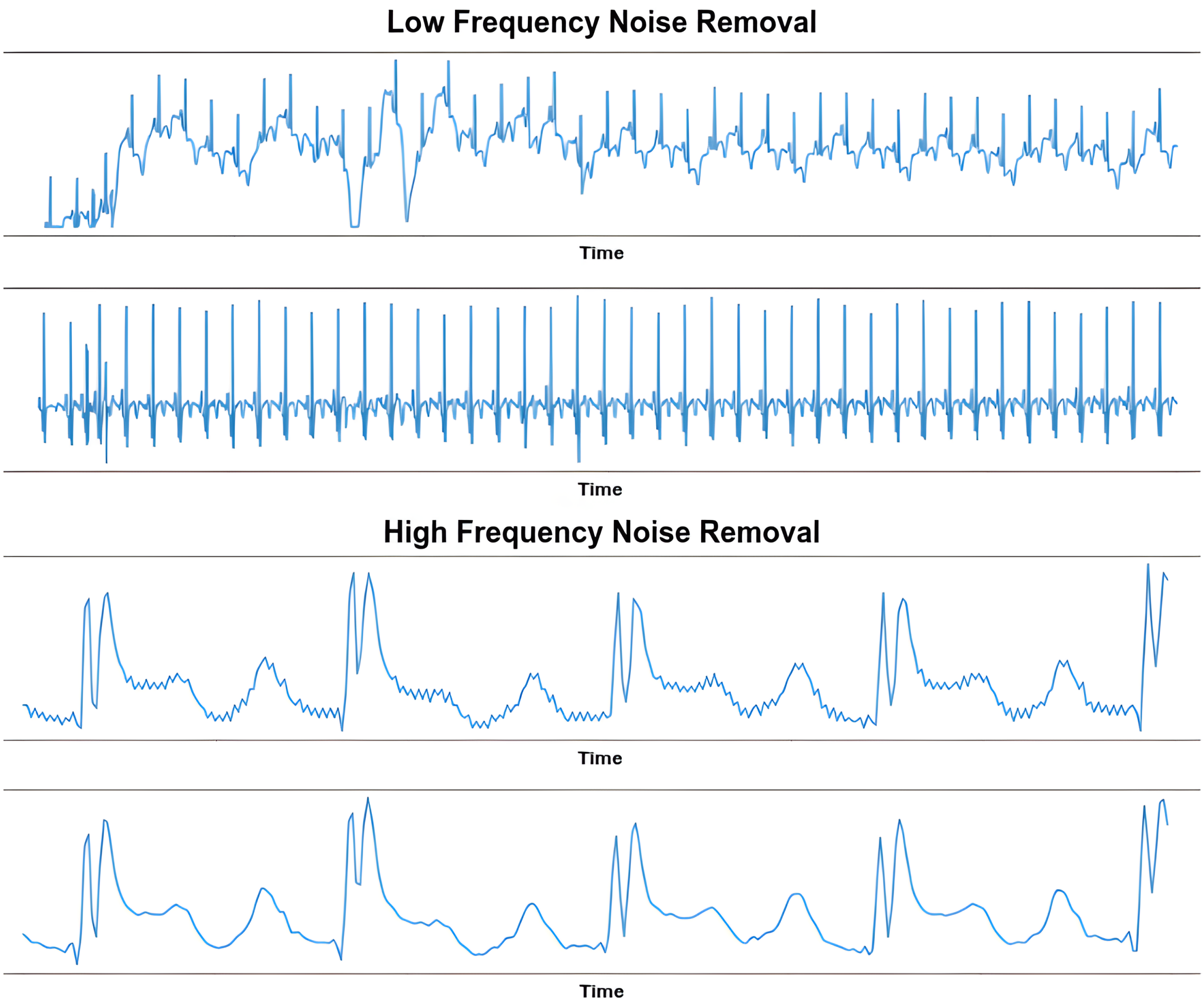

Figure 4.1: Effect of low frequency and high frequency noise removal from the raw ECG signals.

To prepare the data for analysis, we first normalised the ECG and PPG signals to a range of [-1, 1] using MinMaxScaling. The signals were then segmented into 3-second intervals. The preprocessed data was split into an 80-20 training and testing split. Importantly, we ensured that patient data was not included in both the training and testing sets, thereby ensuring that the model was tested on data that it had not been trained on. The training dataset comprised 32529 3-second ECG and PPG segments from 1573 patients, while the test set included 10854 3-second ECG and PPG segments from 394 patients.

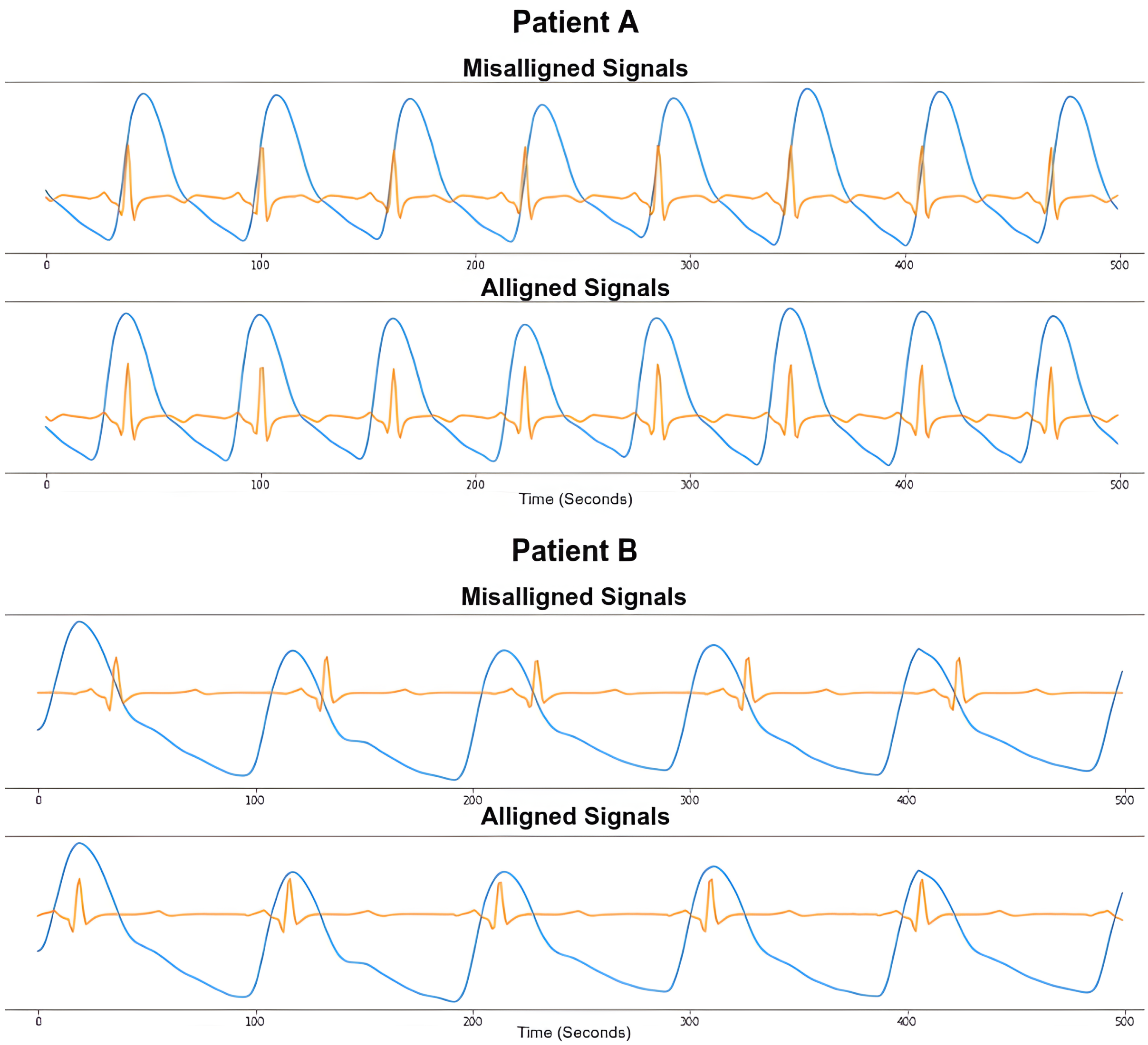

Figure 4.2: PPG and ECG Signal Alignment for two patients.

4.2.2 Model Architecture

4.2.2.1 Encoder-Decoder Network

The proposed encoder-decoder architecture for the autoencoding experiment is illustrated in Figure 4.3. To convert the input signal into its latent space, which can then be decoded back to get the original signal, we used 1D convolutions. The encoder network downscales the input signal to obtain a latent space representation by using multiple 1D Convolutions of stride 2, while the decoder network upscales the latent space representation of the original signal to obtain the prediction of the original signal by using 1D TransposeConvolutions with stride 2. The autoencoder used in the study had four downsampling and four upsampling layers.

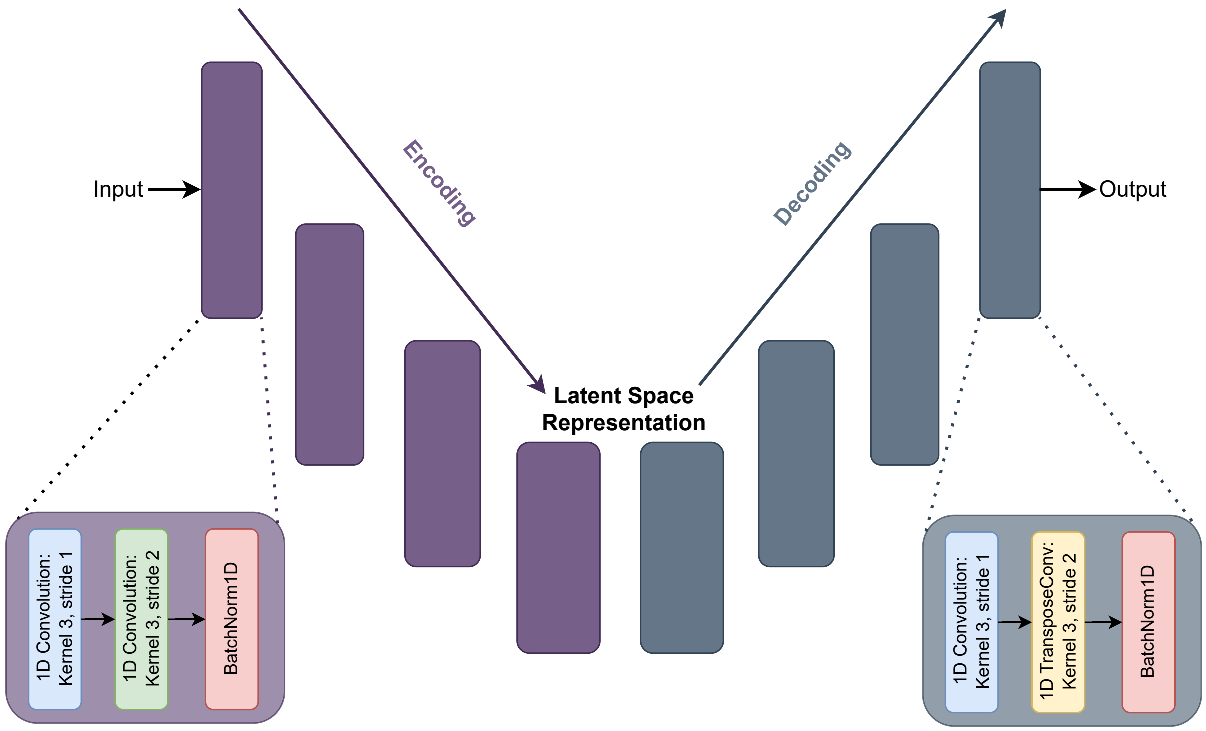

Figure 4.3: Encoder-Decoder Model Architecture.

4.2.2.2 WGAN-GP model for PPG to ECG conversion

In this study, we aimed to generate ECG signals from underlying PPG signals using a Wasserstein GAN with gradient Penalty (WGAN-GP) [48]. WGAN-GP is a powerful variant of traditional GANs, which employs the Wasserstein distance loss function to measure the distance between true and generated data distributions. Unlike the binary cross-entropy loss function used in traditional GANs, Wasserstein distance has been shown to be more effective in training stable and high-quality GANs. Moreover, WGAN-GP employs a gradient penalty technique to improve the stability of training and prevent mode collapse, leading to smoother gradients and more stable training. Thus, WGAN-GP produces more stable and higher quality generated samples compared to traditional GANs.

The WGAN-GP framework requires a generator and discriminator. In our experiment, the generator network was given the original PPG signal as input, and it generated an ECG signal using the inputted PPG. The discriminator network was then provided with either a generated ECG signal or the original ECG signal along with a PPG signal, and it had to determine whether the given ECG signal was from the dataset or generated by the generator network. The networks were trained using a game-theoretic approach, where the discriminator and generator networks competed with each other. Finally, the trained generator network was used to generate the final ECG signal. We utilized three generator networks, namely U-Net [106], Attention U-Net [88], and U-Net++ [161]. Figure 4.4, 4.5 and 4.6 provide a comprehensive overview of the model architecture for each of the networks.

The discriminator network consisted of convolutions to encode the incoming ECG and PPG signals. The encoding was then given to a fully connected neural network to output a binary value indicating whether the inputted ECG signal was generated by generator or not. Refer to Figure 4.7 for a better understanding of the discriminator network.

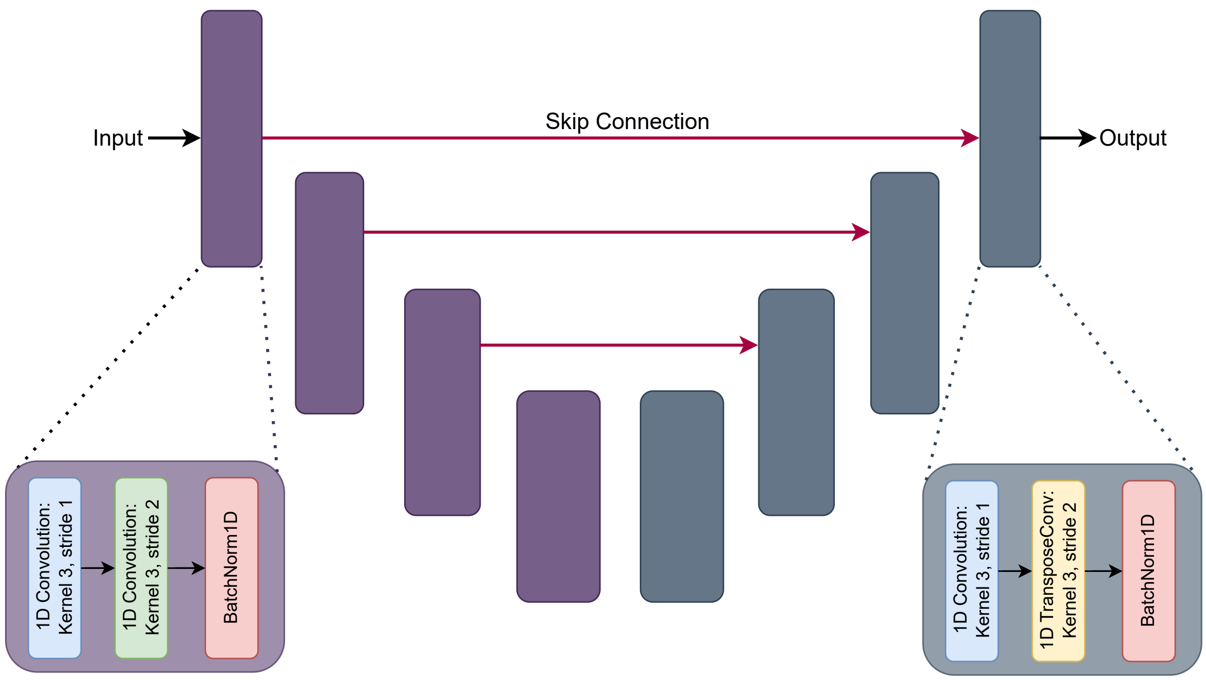

Figure 4.4: U-Net model architecture for the generator. The model consists of a contracting path (left side) and a symmetric expanding path (right side). Skip connections connect corresponding layers in the contracting and expanding paths to help preserve spatial information. The model used had 4 downsampling and 4 upsampling layers.

4.2.3 Model Training and Testing

The machine learning models underwent a training on the training set, utilizing the ADAM optimiser [64]. During the training, a Batch Size of 192 was set. Once training was completed, the model was tested on the hold-out test set using evaluation metrics to evaluate the signal generation quality. The implementation of the model was accomplished using Pytorch version ‘1.12.1’ [96] and an NVIDIA GeForce GTX 3080Ti with 12 GB memory. All other models outlined in the Results and Experiments Section were trained and evaluated following similar procedures. The evaluation metrics used were

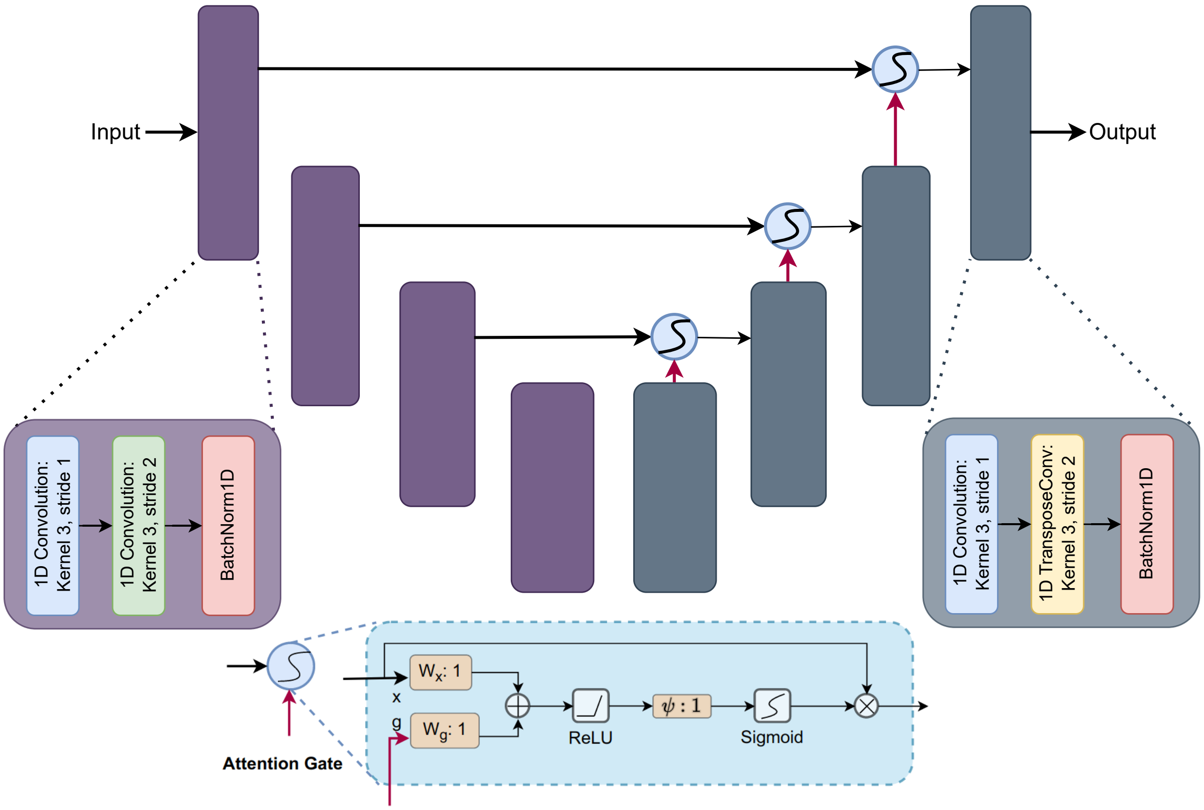

Figure 4.5: Model architecture of Attention U-Net for generator. The generator network consists of an encoder path that progressively downsamples the input image, followed by a decoder path that upsamples the feature maps. Attention blocks are added to the decoder path to selectively enhance the important features.

same as the one explained in Chapter 3. Namely the Mean Squared Error (Equation 3.2) and the Pearson Correlation Coefficient(ρ) (Equation 3.1) were used.

4.3 Experiments and Results

4.3.1 AutoEncoding PPG and ECG

To better understand if encoding and decoding the PPG and ECG signals is possible, we experimented with individually autoencoding the PPG and ECG signals. The Encoder-Decoder model proposed in the Methods section was able to encode and decode the PPG signals with a mean MSE of 0.0000213 and ρ of 0.96. The Encoder-Decodermodel was able to encode and decode the ECG signals with a mean MSE of 0.0000070 and ρ of 0.92. Figure 4.8 can be used to compare the quality of autoencoding the PPG and ECG signals. The autoencoding results suggest that it is possible to encode and

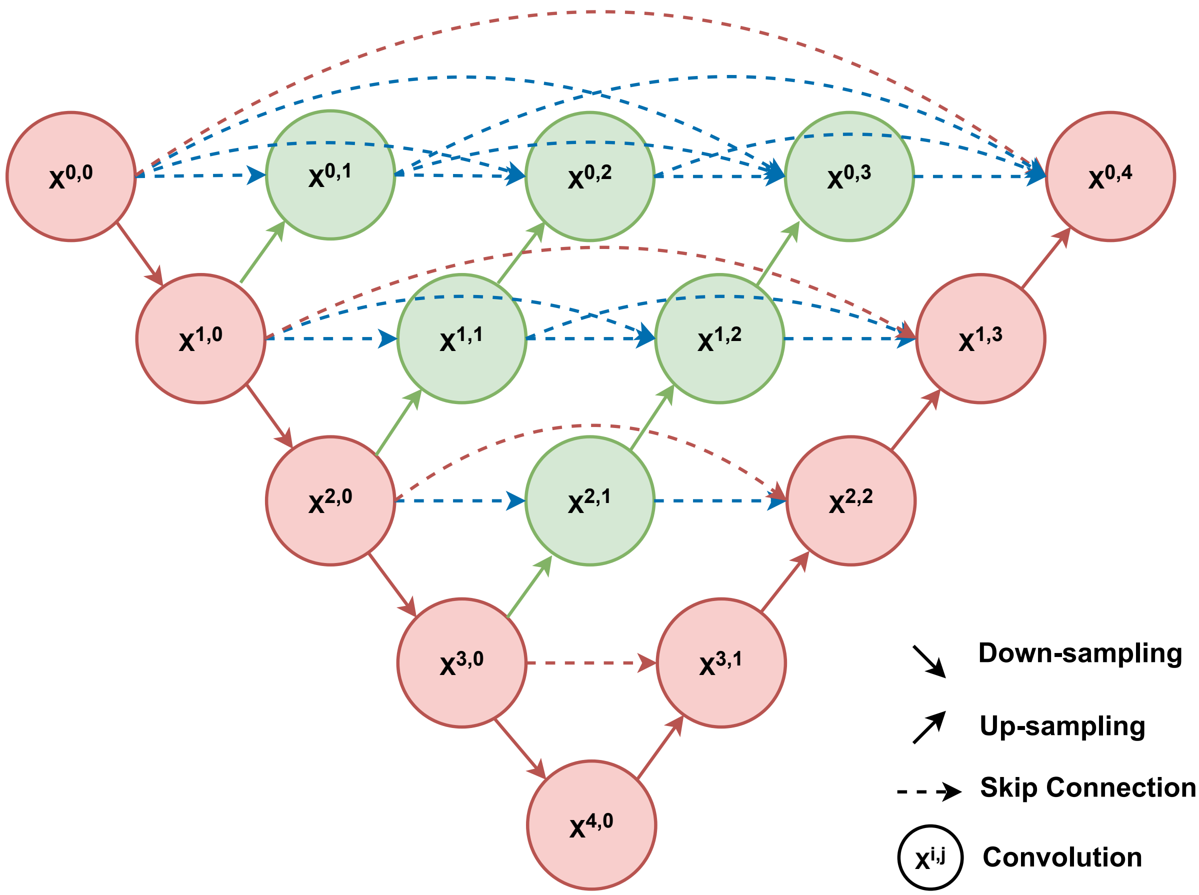

Figure 4.6: U-Net++ model architecture. The U-Net++ architecture extends the original U-Net model by adding nested and dense skip pathways that allow for enhanced performance. In the figure, the red colour is used to identify the original U-Net while the green and blue colours represent the dense skip pathways. For downsampling a 1D convolution with stride 2 and kernel length 3 was used. The upsampling layer utilised a 1D Transpose Convolution with stride 2 and kernel length 3. The convolution block uses the 1D Convolution with kernel length 3 and stride 1.

decode the PPG and ECG signals to and from their respective latent space representations, although the ECG autoencoding results were a bit inferior than the PPG autoencoding results.

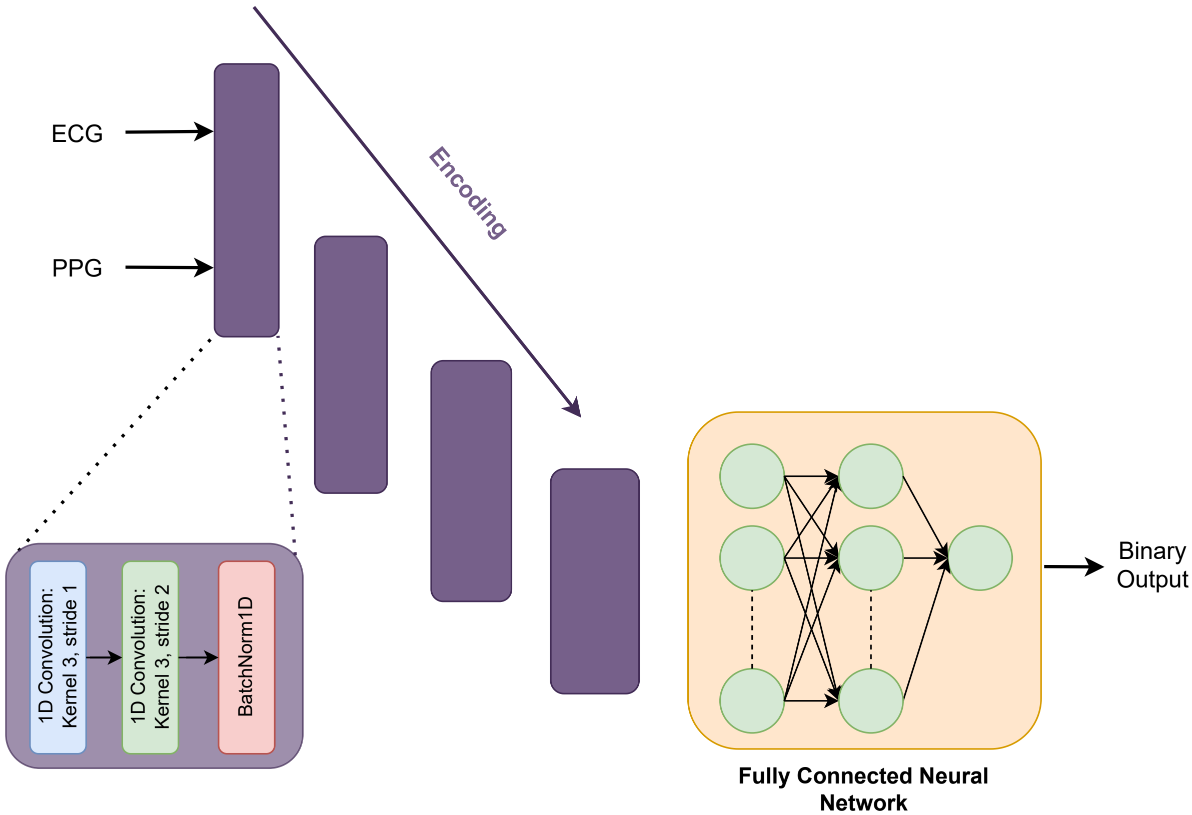

Figure 4.7: Discriminator Model Architecture.The model consists of multiple convolutions to encode the incoming ECG and PPG signals. The encoding is used as an input to Fully Connected Neural Network to get the final binary output.

4.3.2 ECG generation using the underlying PPG signals

We have shown that both PPG and ECG signals can be easily converted back from their respective latent space representations using a deep learning architecture based on the outcomes of the encoding-decoding experiment carried out. We used a variety of CNN-based algorithms to convert the PPG data to an ECG. These networks first converted the input PPG signal to a latent space representation, which was subsequently decoded to produce the corresponding ECG signal. Several models were tested, including the vanilla U-Net and U-Net++. Furthermore, we evaluated the performance of the WGAN-GP with a discriminator architecture, as illustrated in Figure 4.7, and different generator architectures, such as the U-Net, Attention U-Net, and U-Net++. The findings of our models for ECG generation are reported in Table 4.1.

The performance of the different models varied in generating ECG signals from PPG inputs. The vanilla U-Net and U-Net++ models showed poorer performance compared to the GAN based models.

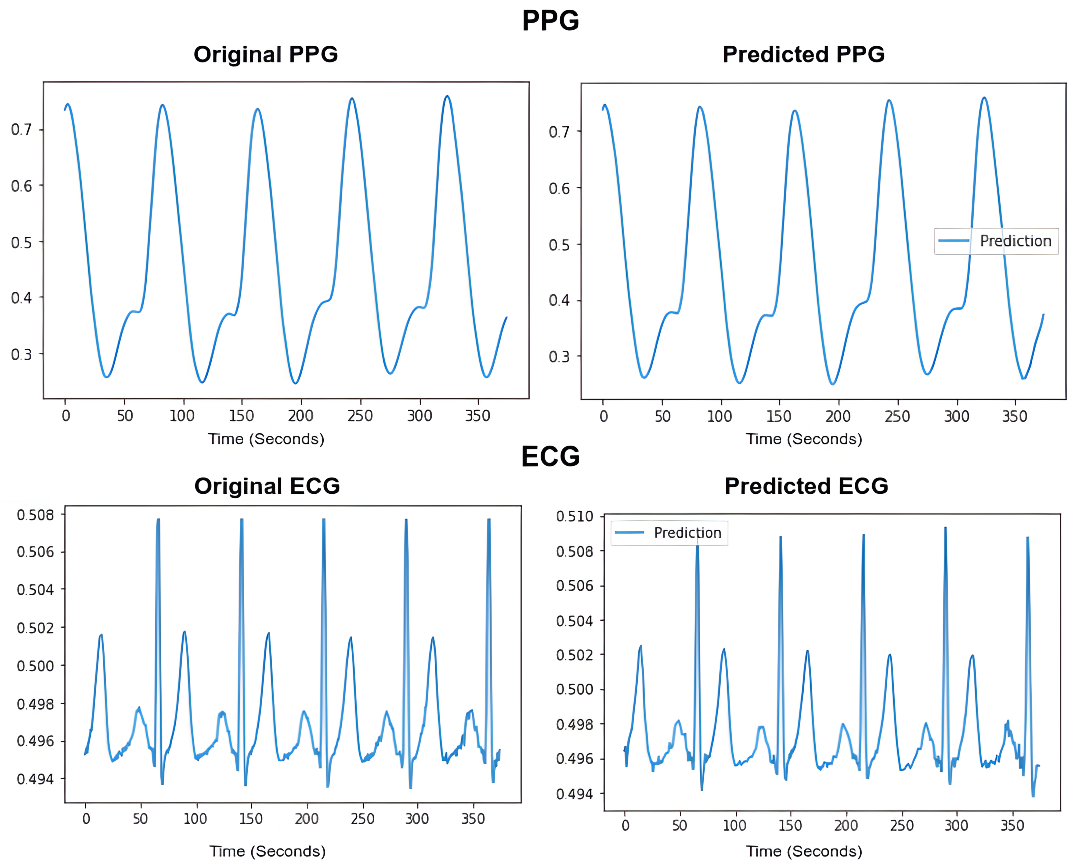

Figure 4.8: Original and Generated PPG and ECG using an Encoder-Decoder Network.

Model	Pearson Correlation Coefficient (ρ)
U-Net	0.09
U-Net++	0.12
WGAN-GP with U-Net as generator (Same as [142])	0.38
WGAN-GP with Attention U-Net as generator	0.43
WGAN-GP with U-Net++ as generator	**0.46**

Table 4.1: Results for ECG generation using PPG for various tested models.

The WGAN-GP with U-Net as the generator model, which is similar to the one used in the study by Vo et al. [142], achieved a correlation coefficient of 0.38. By using an Attention U-Net instead of the U-Net, the model was able to generate ECG signals with a higher correlation coefficient of 0.43. Further improvements were observed by replacing Attention U-Net with U-Net++, resulting in a correlation coefficient of 0.46. However, we should consider that the U-Net++ model significantly increased the number of parameters used by the generator. The generated ECG signals from the WGAN-GP with

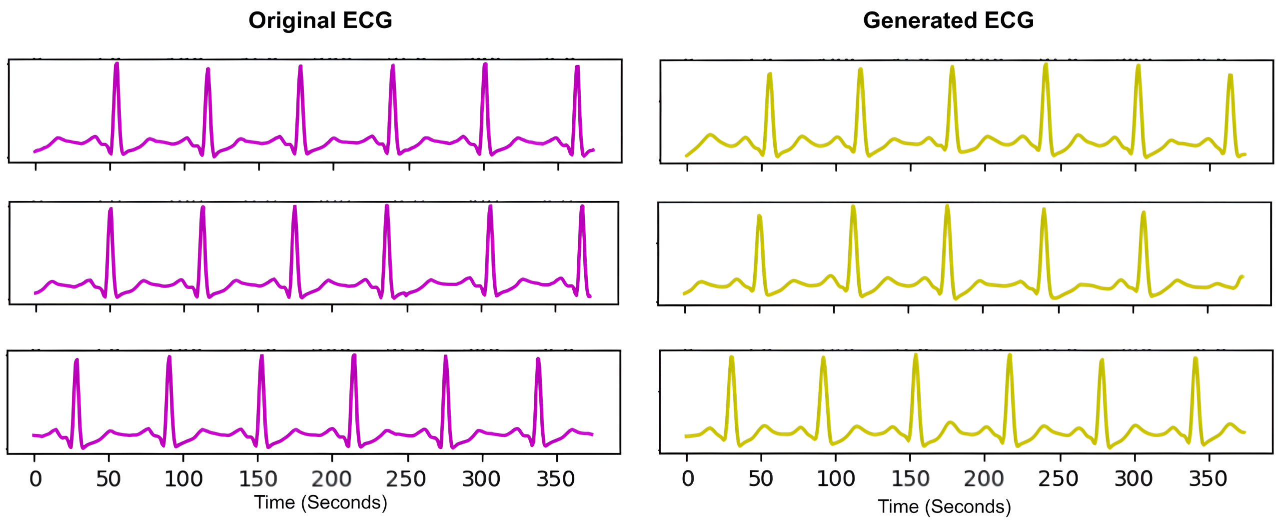

Figure 4.9: Comparison of the Original ECG and ECG signal generated using WGAN-GP with Unet++ as generator.

U-Net++ as the generator model were visually compared to actual ECG signals, as shown in Figure 4.9. We also tested this model in a setting where patient wise segregation of data wasn't ensured, the performance of the model significantly improved from a ρ of 0.46 to 0.72. Thus validating the hypothesis that using the same patient's data for training and testing resulted in inflated results.

4.4 Discussion and Conclusion

ECGs are crucial in making cardiovascular diagnostic decisions, and with the increasing advancements in technology and heightened awareness of health metric tracking, there have been significant innovations in the wearable device sector utilizing ECG signals. However, a major obstacle that device-makers face is the difficulty in collecting ECGs. PPG signals, on the other hand, are easier to collect. However, clinicians trained to diagnose based on ECGs may find it challenging to interpret PPG data. ECG reconstruction primarily aims to bridge this gap between the ease of PPG data collection from modern wearable devices and the consumption of standardized ECG data by clinicians and ECG analysis models. It is essential to note that ECG reconstruction cannot create new ECG data from PPG data. Instead, it converts all the information captured in PPG data into a more interpretable ECG version.

In this chapter, we propose a WGAN-GP model that employs Unet++ as the generator to reconstruct lead II of ECG using PPG signals. Our experimental findings reveal that our proposed model outperforms all other models tested for generating ECG signals, including the one used by Vo et al. Vo et al. reported that their model generated ECG signals with a mean Pearson Correlation Coefficient of 0.835. It is noteworthy that our experimental results for all the models were inferior to those presented by Vo et al.. We tried to reproduce the Vo et al.'s experimentation. It is essential to note that Vo et al. did not use patient-wise segregation of data, hence, to reproduce the study, we also did not use patient-wise segregation of data. Despite multiple efforts to reproduce their results, we found that their results were unreproducible. Our best attempt at reproducing their results resulted in a mean Pearson Correlation Coefficient of 0.593, which is considerably lower than the reported value. We also tested the Vo et al.'s model using patient-wise segregation, and the performance declined to a ρ of 0.382. We conducted all the experiments using patient-wise segregation of data for training and testing, which could have been a major reason for poorer performance of the model in our analysis compared to past studies. Unfortunately, the authors did not respond to our inquiries, and we decided not to move further with the project.

Our research has been limited to the generation of a single lead ECG from underlying PPG signals, which provides only a partial view of the heart's electrical activity. As discussed in Chapter 3, the 12-lead ECG is considered the gold standard for clinical diagnosis. Therefore, future research efforts should focus on generating 12-lead ECG from PPG signals to provide a better picture of the electrical activity of heart. Furthermore, our models were tested on a single cohort of data, and the results may not be generalizable to other cohorts due to varying factors among the two cohorts. The application of data-intensive models like transformers [138] could improve ECG synthesis using PPG signals, leading to further advancements in the field.

Chapter 5

Summary and Future Directions

Cardiology is a crucial field in medicine that deals with the prevention, diagnosis, and treatment of various heart-related conditions, including cardiovascular diseases, a leading cause of mortality worldwide. AI has shown great potential in managing these diseases, as it can assist physicians in the diagnosis and treatment of cardiac conditions by providing more accurate and efficient analyses of patient data. Additionally, AI can help predict patient outcomes and determine the most appropriate treatment options for individual patients. Despite reduced lead set ECG and PPG data being easier to collect, conventional medical infrastructure is heavily dependent on the 12-lead ECG, creating a gap between the ease of collecting data and the ability to process it. To address this issue, we propose a Deep Learning-based solution to generate 12-lead ECG data using single-lead ECG and single-lead ECG data using the PPG signals. Our proposed solution aims to improve the accessibility and accuracy of cardiac monitoring, ultimately leading to better healthcare outcomes.

Chapter 3 presents a novel approach to reconstructing the 12-lead ECG using only the lead II ECG signal. The proposed method involves a modified attention U-Net, which is capable of generating all 12 leads at once, leading to improved model performance and reduced computational overhead compared to previous studies. Furthermore, unlike previous works that only reconstructed small ECG segments, our approach is trained to reconstruct longer 10-second ECG signals. The model's real-life utility is demonstrated by using it for cardiovascular disease classification, unlike the evaluation metrics used to asses the signal generation quality the experiment helps in understanding if the model is able to maintain the artifacts necessary for accurate disease diagnosis.

Chapter 4 of the thesis introduces a novel approach for converting PPG signals into single-lead ECG signals, using a Wasserstein generative adversarial network. Unlike previous studies, we use longer 3-second PPG segments to generate a complete 3-second ECG signal in one step. The chapter also highlights a significant limitation in earlier studies, where same patient's data was used for both model training and testing. To address this issue, we employ patient-specific data segmentation, resulting in more reliable results.

The use of data from a single cohort in both Chapter 3 and Chapter 4 can limit the generalisability of results. To obtain more reliable results, it is necessary to conduct extensive studies involving patients from multiple cohorts. The increasing digitisation of healthcare data may facilitate the use of data-intensive models like transformers to enhance the accuracy and robustness of such studies. Chapter 4 of the thesis focuses only on the generation of single-lead ECG from PPG data. However, it should be considered that the 12-lead ECG data is considered the gold standard for cardiac diagnosis, therefore, another promising direction for future research is the generation of 12-lead ECG data from PPG data. While PPG data collection is relatively easy, it may not provide a complete picture of cardiac health. We can combine PPG data with lead II ECG data to get a better picture of heart's activity. This approach may result in better 12-lead ECG data generation, as it combines the strengths of both PPG and lead II ECG data. Overall, the a collection of data from several sources and the use of advanced models can enhance the accuracy and clinical utility of cardiac diagnostic tools.

Although there are many obstacles to overcome for the regular utilisation of AI in healthcare, we remain optimistic about its potential to transform the industry. We envision AI as a valuable tool for assisting healthcare professionals, rather than replacing them entirely. By working alongside radiologists and clinicians, AI has the potential to provide more efficient and cost-effective medical care to patients, regardless of their geographic location. As AI continues to evolve, it will likely be capable of assisting with a wide range of healthcare tasks, including diagnosing diseases, monitoring vital signs, and even predicting potential health risks before they manifest into more significant issues. However, AI should not be seen as a complete replacement for human expertise and intervention, as there will always be a need for a human touch in healthcare. In conclusion, it is our belief that AI has the ability to bring significant positive change to the healthcare sector, but it is crucial to approach its implementation with caution and care to ensure its safe and effective use.

Related Publications

1. Akshaya Karthikeyan†, **Akshit Garg**†, and U. Deva Priyakumar. "Machine learning based clinicaldecision support system for early COVID-19 mortality prediction" *Frontiers in Public Health.* 2021; 9.

2. Shanmukh Alle†, Samreen Siddiqui†, Akshay Kanakan†, **Akshit Garg**†, Akshaya Karthikeyan†, Neha Mishra, Swati Waghdhare, Akansha Tyagi, Bansidhar Tarai, Pranjal Pratim Hazarika, Poonam Das, Sandeep Budhiraja, Vivek Nangia, Arun Dewan, Ramanathan Sethuraman, C. Subramanian, Mashrin Srivastava, Avinash Chakravarthi, Johnny Jacob, Madhuri Namagiri, Varma Konala, Debasish Dash, Sujeet Jha, Rajesh Pandey, Anurag Agrawal, P. K. Vinod, and U. Deva Priyakumar. "COVID-19 Risk Stratification and Mortality Prediction in Hospitalized Indian Patients: Harnessing clinical data for public health benefits" *PLoS One* 17.3 (2022): e0264785.

3. **Akshit Garg**†, Vijay Vignesh Venkataranami†, Akshaya Karthikeyan, and U. Deva Priyakumar "Modern AI/ML Methods for Healthcare: Opportunities and Challenges." *Distributed Computing and Intelligent Technology: 18th International Conference*, ICDCIT 2022, Bhubaneswar, India, January 19–23, 2022, Proceedings. Cham: Springer International Publishing, 2022.

4. Divya B. Korlepara, C. S. Vasavi, Shruti Jeurkar, Pradeep Kumar Pal, Subhajit Roy, Sarvesh Mehta, Shubham Sharma, Vishal Kumar, Charuvaka Muvva, Bhuvanesh Sridharan, **Akshit Garg**, Rohit Modee, Agastya P. Bhati, Divya Nayar, and U. Deva Priyakumar "Plas-5k: Dataset of protein-ligand affinities from molecular dynamics for machine learning applications." *Scientific Data* 9.1 (2022): 548.

5. Vijay Vignesh Venkataramani †, **Akshit Garg** †, and U. Deva Priyakumar. "Modified Variable Kernel Length ResNets for Heart Murmur Detection and Clinical Outcome Prediction using Multi-positional Phonocardiogram Recording." *Computing in Cardiology, 2022*

6. **Akshit Garg**, Vijay Vignesh Venkataramani, and U. Deva Priyakumar. "Single-Lead to Multi-Lead Electrocardiogram Reconstruction Using a Modified Attention U-Net Framework" Accepted in *International Joint Conference on Neural Networks, IJCNN 2023*

7. Akshaya Karthikeyan, Shanmukh Alle, **Akshit Garg**, Vijay Vignesh Venkataramani, and U. Deva Priyakumar. "FXD Score: An Improved Metric for Evaluating Chest X-Ray Generation Methods" *In Review*

† **signifies first co-authorship**

Bibliography

[1] E. D. Adler, A. A. Voors, L. Klein, F. Macheret, O. O. Braun, M. A. Urey, W. Zhu, I. Sama, M. Tadel, C. Campagnari, et al. Improving risk prediction in heart failure using machine learning. *European journal of heart failure*, 22(1):139–147, 2020. 10

[2] S. Ajay and P. Deshpande. Preventive readmission in hospitals using machine learning. In *2020 IEEE International Conference for Innovation in Technology (INOCON)*, pages 1–5. IEEE, 2020. 11

[3] A. Akella and S. Akella. Machine learning algorithms for predicting coronary artery disease: efforts toward an open source solution. *Future science OA*, 7(6):FSO698, 2021. 1, 6

[4] H. Alfalahi, F. Renda, and C. Stefanini. Concentric tube robots for minimally invasive surgery: Current applications and future opportunities. *IEEE Transactions on Medical Robotics and Bionics*, 2(3):410–424, 2020. 11

[5] A. A. Alian and K. H. Shelley. Photoplethysmography. *Best Practice & Research Clinical Anaesthesiology*, 28(4):395–406, 2014. 28

[6] S. Alle and U. Priyakumar. Linear prediction residual for efficient diagnosis of parkinson's disease from gait. In *International Conference on Medical Image Computing and Computer-Assisted Intervention*, pages 614–623. Springer, 2021. 8

[7] H. S. AlSagri and M. Ykhlef. Machine learning-based approach for depression detection in twitter using content and activity features. *IEICE Transactions on Information and Systems*, 103(8):1825–1832, 2020. 8

[8] J. D. Álvarez, J. A. Matias-Guiu, M. N. Cabrera-Martín, J. L. Risco-Martín, and J. L. Ayala. An application of machine learning with feature selection to improve diagnosis and classification of neurodegenerative disorders. *BMC bioinformatics*, 20(1):1–12, 2019. 8

[9] M. Aly, K. H. Rahouma, and S. M. Ramzy. Pay attention to the speech: Covid-19 diagnosis using machine learning and crowdsourced respiratory and speech recordings. *Alexandria Engineering Journal*, 2021. 12

[10] S. F. Ardabili, A. Mosavi, P. Ghamisi, F. Ferdinand, A. R. Varkonyi-Koczy, U. Reuter, T. Rabczuk, and P. M. Atkinson. Covid-19 outbreak prediction with machine learning. *Algorithms*, 13(10):249, 2020. 12

[11] M. Arjovsky, S. Chintala, and L. Bottou. Wasserstein generative adversarial networks. In *International conference on machine learning*, pages 214–223. PMLR, 2017. 29

[12] S. Asif and Y. Wenhui. Automatic detection of covid-19 using x-ray images with deep convolutional neural networks and machine learning. *medRxiv*, 2020. 12

[13] S. Asif, Y. Wenhui, Y. Tao, S. Jinhai, and K. Amjad. Real time face mask detection system using transfer learning with machine learning method in the era of covid-19 pandemic. In *2021 4th International Conference on Artificial Intelligence and Big Data (ICAIBD)*, pages 70–75. IEEE, 2021. 12

[14] L. Aversano, M. L. Bernardi, M. Cimitile, and R. Pecori. Early detection of parkinson disease using deep neural networks on gait dynamics. In *2020 International Joint Conference on Neural Networks (IJCNN)*, pages 1–8. IEEE, 2020. 8

[15] D. Bahdanau, K. Cho, and Y. Bengio. Neural machine translation by jointly learning to align and translate. *arXiv preprint arXiv:1409.0473*, 2014. 22

[16] M. Barstugan, U. Ozkaya, and S. Ozturk. Coronavirus (covid-19) classification using ct images by machine learning methods. *arXiv preprint arXiv:2003.09424*, 2020. 12

[17] S. K. Berkaya, A. K. Uysal, E. S. Gunal, S. Ergin, S. Gunal, and M. B. Gulmezoglu. A survey on ecg analysis. *Biomedical Signal Processing and Control*, 43:216–235, 2018. 15

[18] H. Binol, A. Plotner, J. Sopkovich, B. Kaffenberger, M. K. K. Niazi, and M. N. Gurcan. Ros-net: A deep convolutional neural network for automatic identification of rosacea lesions. *Skin Research and Technology*, 26(3):413–421, 2020. 7

[19] J. S. Bobby and C. Annapoorani. Analysis of intracranial hemorrhage in ct brain images using machine learning and deep learning algorithm. *Annals of the Romanian Society for Cell Biology*, 25(6):13742–13752, 2021. 8

[20] C. Boeri, C. Chiappa, F. Galli, V. De Berardinis, L. Bardelli, G. Carcano, and F. Rovera. Machine learning techniques in breast cancer prognosis prediction: A primary evaluation. *Cancer medicine*, 9(9):3234–3243, 2020. 9

[21] S. Bolourani, M. Brenner, P. Wang, T. McGinn, J. S. Hirsch, D. Barnaby, T. P. Zanos, N. C.-. R. Consortium, et al. A machine learning prediction model of respiratory failure within 48 hours of patient admission for covid-19: model development and validation. *Journal of medical Internet research*, 23(2):e24246, 2021. 12

[22] A. C. Brewer, D. C. Endly, J. Henley, M. Amir, B. P. Sampson, J. F. Moreau, and R. P. Dellavalle. Mobile applications in dermatology. *JAMA dermatology*, 149(11):1300–1304, 2013. 7

[23] L. Brunese, F. Mercaldo, A. Reginelli, and A. Santone. An ensemble learning approach for brain cancer detection exploiting radiomic features. *Computer methods and programs in biomedicine*, 185:105134, 2020. 8

[24] M. C. d. Bruyne, J. A. Kors, A. W. Hoes, P. Klootwijk, J. M. Dekker, A. Hofman, J. H. van Bemmel, and D. E. Grobbee. Both decreased and increased heart rate variability on the standard 10-second electrocardiogram predict cardiac mortality in the elderly: the rotterdam study. *American journal of epidemiology*, 150(12):1282–1288, 1999. 16

[25] R. Buettner, M. Hirschmiller, K. Schlosser, M. Rössle, M. Fernandes, and I. J. Timm. High-performance exclusion of schizophrenia using a novel machine learning method on eeg data. In *2019 IEEE International Conference on E-health Networking, Application & Services (HealthCom)*, pages 1–6. IEEE, 2019. 8

[26] J. J. Chabon, E. G. Hamilton, D. M. Kurtz, M. S. Esfahani, E. J. Moding, H. Stehr, J. Schroers-Martin, B. Y. Nabet, B. Chen, A. A. Chaudhuri, et al. Integrating genomic features for non-invasive early lung cancer detection. *Nature*, 580(7802):245–251, 2020. 8

[27] A. Cheerla and O. Gevaert. Deep learning with multimodal representation for pancancer prognosis prediction. *Bioinformatics*, 35(14):i446–i454, 2019. 9

[28] H.-Y. Chiu, H.-H. Shuai, and P. C.-P. Chao. Reconstructing qrs complex from ppg by transformed attentional neural networks. *IEEE Sensors Journal*, 20(20):12374–12383, 2020. 29

[29] A. Christe, A. A. Peters, D. Drakopoulos, J. T. Heverhagen, T. Geiser, T. Stathopoulou, S. Christodoulidis, M. Anthimopoulos, S. G. Mougiakakou, and L. Ebner. Computer-aided diagnosis of pulmonary fibrosis using deep learning and ct images. *Investigative radiology*, 54(10):627, 2019. 7

[30] E. K. Chung. *Ambulatory electrocardiography: holter monitor electrocardiography*. Springer Science & Business Media, 2013. 15

[31] J. P. Cohen, L. Dao, K. Roth, P. Morrison, Y. Bengio, A. F. Abbasi, B. Shen, H. K. Mahsa, M. Ghassemi, H. Li, et al. Predicting covid-19 pneumonia severity on chest x-ray with deep learning. *Cureus*, 12(7), 2020. 13

[32] P. S. Dammu and R. S. Bapi. Employing temporal properties of brain activity for classifying autism using machine learning. In *International Conference on Pattern Recognition and Machine Intelligence*, pages 193–200. Springer, 2019. 8

[33] P. S. Dammu and R. S. Bapi. Temporal dynamics of the brain using variational bayes hidden markov models: Application in autism. In *International Conference on Pattern Recognition and Machine Intelligence*, pages 121–130. Springer, 2019. 8

[34] S. Daud and R. Sudirman. Butterworth bandpass and stationary wavelet transform filter comparison for electroencephalography signal. In *2015 6th International Conference on Intelligent Systems, Modelling and Simulation*, pages 123–126. IEEE, 2015. 17, 30

[35] M. Deshpande and V. Rao. Depression detection using emotion artificial intelligence. In *2017 international conference on intelligent sustainable systems (iciss)*, pages 858–862. IEEE, 2017. 8

[36] G.-P. Diller, A. Kempny, S. V. Babu-Narayan, M. Henrichs, M. Brida, A. Uebing, A. E. Lammers, H. Baumgartner, W. Li, S. J. Wort, et al. Machine learning algorithms estimating prognosis and guiding therapy in adult congenital heart disease: data from a single tertiary centre including 10 019 patients. *European heart journal*, 40(13):1069–1077, 2019. 1

[37] P. I. Dorado-Díaz, J. Sampedro-Gómez, V. Vicente-Palacios, and P. L. Sánchez. Applications of artificial intelligence in cardiology. the future is already here. *Revista Española de Cardiología (English Edition)*, 72(12):1065–1075, 2019. 1

[38] M. C. T. Dos Santos, M. A. Barreto-Sanz, B. R. S. Correia, R. Bell, C. Widnall, L. T. Perez, C. Berteau, C. Schulte, D. Scheller, D. Berg, et al. mirna-based signatures in cerebrospinal fluid as potential diagnostic tools for early stage parkinson's disease. *Oncotarget*, 9(25):17455, 2018. 8

[39] V. Dumoulin and F. Visin. A guide to convolution arithmetic for deep learning. *arXiv preprint arXiv:1603.07285*, 2016. 18

[40] J. O. Emuoyibofarhe, D. Ajisafe, R. S. Babatunde, and M. Christoph. Early skin cancer detection using deep convolutional neural networks on mobile smartphone. *International Journal of Information Engineering & Electronic Business*, 12(2), 2020. 8

[41] A. Esteva, B. Kuprel, R. A. Novoa, J. Ko, S. M. Swetter, H. M. Blau, and S. Thrun. Dermatologist-level classification of skin cancer with deep neural networks. *nature*, 542(7639):115–118, 2017. 7, 8

[42] V. Flenady, L. Koopmans, P. Middleton, J. F. Frøen, G. C. Smith, K. Gibbons, M. Coory, A. Gordon, D. Ellwood, H. D. McIntyre, et al. Major risk factors for stillbirth in high-income countries: a systematic review and meta-analysis. *The lancet*, 377(9774):1331–1340, 2011. 10

[43] T. B. Garcia. *12-lead ECG: The art of interpretation*. Jones & Bartlett Publishers, 2013. 15

[44] A. L. Goldberger, L. A. Amaral, L. Glass, J. M. Hausdorff, P. C. Ivanov, R. G. Mark, J. E. Mietus, G. B. Moody, C.-K. Peng, and H. E. Stanley. Physiobank, physiotoolkit, and physionet: components of a new research resource for complex physiologic signals. *circulation*, 101(23):e215–e220, 2000. 30

[45] P. Gomes. Surgical robotics: Reviewing the past, analysing the present, imagining the future. *Robotics and Computer-Integrated Manufacturing*, 27(2):261–266, 2011. 11

[46] V. Gomez. The use of butterworth filters for trend and cycle estimation in economic time series. *Journal of Business & Economic Statistics*, 19(3):365–373, 2001. 17, 30

[47] I. Goodfellow, J. Pouget-Abadie, M. Mirza, B. Xu, D. Warde-Farley, S. Ozair, and Y. Bengio. Generative adversarial networks, 1–9. *arXiv preprint arXiv:1406.2661*, 2014. 29

[48] I. Gulrajani, F. Ahmed, M. Arjovsky, V. Dumoulin, and A. C. Courville. Improved training of wasserstein gans. *Advances in neural information processing systems*, 30, 2017. 29, 33

[49] V. Gundlapalle and A. Acharyya. A novel single lead to 12-lead ecg reconstruction methodology using convolutional neural networks and lstm. In *2022 IEEE 13th Latin America Symposium on Circuits and System (LASCAS)*, pages 01–04. IEEE, 2022. 16, 22

[50] E. Gustafson, J. Pacheco, F. Wehbe, J. Silverberg, and W. Thompson. A machine learning algorithm for identifying atopic dermatitis in adults from electronic health records. In *2017 IEEE International Conference on Healthcare Informatics (ICHI)*, pages 83–90. IEEE, 2017. 7

[51] L. Hadzievski, B. Bojovic, V. Vukˇcevic, P. Belicev, S. Pavlovic, Z. Vasiljevic-Pokrajˇcic, and M. Ostojic. A novel mobile transtelephonic system with synthesized 12-lead ecg. *IEEE transactions on information technology in biomedicine*, 8(4):428–438, 2004. 15

[52] F. Hatib, Z. Jian, S. Buddi, C. Lee, J. Settels, K. Sibert, J. Rinehart, and M. Cannesson. Machine-learning algorithm to predict hypotension based on high-fidelity arterial pressure waveform analysis. *Anesthesiology*, 129(4):663–674, 2018. 11

[53] L. Hussain, I. A. Awan, W. Aziz, S. Saeed, A. Ali, F. Zeeshan, and K. S. Kwak. Detecting congestive heart failure by extracting multimodal features and employing machine learning techniques. *BioMed research international*, 2020, 2020. 1, 6

[54] M. Islam, V. J. M. Jose, and H. Ren. Glioma prognosis: Segmentation of the tumor and survival prediction using shape, geometric and clinical information. In *International MICCAI Brainlesion Workshop*, pages 142–153. Springer, 2018. 9

[55] M. R. Islam, M. A. Kabir, A. Ahmed, A. R. M. Kamal, H. Wang, and A. Ulhaq. Depression detection from social network data using machine learning techniques. *Health information science and systems*, 6(1):1–12, 2018. 8

[56] H. Jiang, H. Mao, H. Lu, P. Lin, W. Garry, H. Lu, G. Yang, T. H. Rainer, and X. Chen. Machine learning-based models to support decision-making in emergency department triage for patients with suspected cardiovascular disease. *International Journal of Medical Informatics*, 145:104326, 2021. 11

[57] K. Jnawali, M. R. Arbabshirani, N. Rao, and A. A. Patel. Deep 3d convolution neural network for ct brain hemorrhage classification. In *Medical Imaging 2018: Computer-Aided Diagnosis*, volume 10575, page 105751C. International Society for Optics and Photonics, 2018. 8

[58] A. E. Johnson, T. J. Pollard, L. Shen, L.-w. H. Lehman, M. Feng, M. Ghassemi, B. Moody, P. Szolovits, L. Anthony Celi, and R. G. Mark. Mimic-iii, a freely accessible critical care database. *Scientific data*, 3(1):1–9, 2016. 29

[59] A. Kapfo, S. Datta, S. Dandapat, and P. K. Bora. Lstm based synthesis of 12-lead ecg signal from a reduced lead set. In *2022 IEEE International Conference on Signal Processing, Informatics, Communication and Energy Systems (SPICES)*, volume 1, pages 296–301. IEEE, 2022. 15, 16

[60] S. H. Kassania, P. H. Kassanib, M. J. Wesolowskic, K. A. Schneidera, and R. Detersa. Automatic detection of coronavirus disease (covid-19) in x-ray and ct images: a machine learning based approach. *Biocybernetics and Biomedical Engineering*, 41(3):867–879, 2021. 12

[61] D. Kauffman. Cardiovascular disease burden, deaths are rising around the world. *American College of Cardiology*, 9, 2020. 15

[62] N. Khuriwal and N. Mishra. Breast cancer detection from histopathological images using deep learning. In *2018 3rd international conference and workshops on recent advances and innovations in engineering (ICRAIE)*, pages 1–4. IEEE, 2018. 8

[63] Y. J. Kim, S. S. Han, H. J. Yang, and S. E. Chang. Prospective, comparative evaluation of a deep neural network and dermoscopy in the diagnosis of onychomycosis. *Plos one*, 15(6):e0234334, 2020. 7

[64] D. P. Kingma and J. Ba. Adam: A method for stochastic optimization. *arXiv preprint arXiv:1412.6980*, 2014. 19, 34

[65] E. Klang, Y. Barash, S. Soffer, S. Bechler, Y. S. Resheff, T. Granot, M. Shahar, M. Klug, G. Guralnik, E. Zimlichman, et al. Promoting head ct exams in the emergency department triage using a machine learning model. *Neuroradiology*, 62(2):153–160, 2020. 11

[66] B. P. Knight, F. Pelosi, G. F. Michaud, S. A. Strickberger, and F. Morady. Physician interpretation of electrocardiographic artifact that mimics ventricular tachycardia. *The American journal of medicine*, 110(5):335–338, 2001. 2, 14

[67] G. Kong, K. Lin, and Y. Hu. Using machine learning methods to predict in-hospital mortality of sepsis patients in the icu. *BMC medical informatics and decision making*, 20(1):1–10, 2020. 9

[68] Y.-H. Lai, W.-N. Chen, T.-C. Hsu, C. Lin, Y. Tsao, and S. Wu. Overall survival prediction of non-small cell lung cancer by integrating microarray and clinical data with deep learning. *Scientific reports*, 10(1):1–11, 2020. 9

[69] Y. Li, X. Tian, Q. Zhu, and M. Wu. A lightweight neural network for inferring ecg and diagnosing cardiovascular diseases from ppg. *arXiv preprint arXiv:2012.04949*, 2020. 29

[70] D. Liu, M. Görges, and S. A. Jenkins. University of queensland vital signs dataset: development of an accessible repository of anesthesia patient monitoring data for research. *Anesthesia & Analgesia*, 114(3):584–589, 2012. 29

[71] L. Liu, S. Zhao, H. Chen, and A. Wang. A new machine learning method for identifying alzheimer's disease. *Simulation Modelling Practice and Theory*, 99:102023, 2020. 8

[72] M. Loey, G. Manogaran, M. H. N. Taha, and N. E. M. Khalifa. A hybrid deep transfer learning model with machine learning methods for face mask detection in the era of the covid-19 pandemic. *Measurement*, 167:108288, 2021. 12

[73] F. Lopez-Jimenez, Z. Attia, A. M. Arruda-Olson, R. Carter, P. Chareonthaitawee, H. Jouni, S. Kapa, A. Lerman, C. Luong, J. R. Medina-Inojosa, et al. Artificial intelligence in cardiology: present and future. In *Mayo Clinic Proceedings*, volume 95, pages 1015–1039. Elsevier, 2020. 1

[74] N. Ludwig, T. Fehlmann, F. Kern, M. Gogol, W. Maetzler, S. Deutscher, S. Gurlit, C. Schulte, A.-K. Von Thaler, C. Deuschle, et al. Machine learning to detect alzheimer's disease from circulating non-coding rnas. *Genomics, proteomics & bioinformatics*, 17(4):430–440, 2019. 8

[75] G. Lugli, A. M. Cohen, D. A. Bennett, R. C. Shah, C. J. Fields, A. G. Hernandez, and N. R. Smalheiser. Plasma exosomal mirnas in persons with and without alzheimer disease: altered expression and prospects for biomarkers. *PloS one*, 10(10):e0139233, 2015. 8

[76] T. K. Lui, K.-S. Cheung, and K. L. Lui. Machine learning models in the prediction of one-year mortality in patients with advanced hepatocellular cancer on immunotherapy. *Available at SSRN 3885156*, 2021. 9

[77] S. M. Lundberg, B. Nair, M. S. Vavilala, M. Horibe, M. J. Eisses, T. Adams, D. E. Liston, D. K.-W. Low, S.-F. Newman, J. Kim, et al. Explainable machine-learning predictions for the prevention of hypoxaemia during surgery. *Nature biomedical engineering*, 2(10):749–760, 2018. 11

[78] E. J. d. S. Luz, W. R. Schwartz, G. Cámara-Chávez, and D. Menotti. Ecg-based heartbeat classification for arrhythmia detection: A survey. *Computer methods and programs in biomedicine*, 127:144–164, 2016. 2, 14, 28

[79] M. S. Mahmoud. *Advanced control design with application to electromechanical systems*. Butterworth-Heinemann, 2018. 15

[80] T. Mahmud, M. J. Alam, S. Chowdhury, S. N. Ali, M. M. Rahman, S. A. Fattah, and M. Saquib. Covtanet: A hybrid tri-level attention-based network for lesion segmentation, diagnosis, and severity prediction of covid-19 chest ct scans. *IEEE Transactions on Industrial Informatics*, 17(9):6489–6498, 2020. 13

[81] E. Malacova, S. Tippaya, H. D. Bailey, K. Chai, B. M. Farrant, A. T. Gebremedhin, H. Leonard, M. L. Marinovich, N. Nassar, A. Phatak, et al. Stillbirth risk prediction using machine learning for a large cohort of births from western australia, 1980–2015. *Scientific reports*, 10(1):1–8, 2020. 10

[82] E. A. Mohammed, M. Keyhani, A. Sanati-Nezhad, S. H. Hejazi, and B. H. Far. An ensemble learning approach to digital corona virus preliminary screening from cough sounds. *Scientific Reports*, 11(1):1–11, 2021. 12

[83] A. Monk, K. Harris, N. Donnolley, L. Hilder, M. Humphrey, A. Gordon, and G. Chambers. Perinatal deaths in australia 1993–2012. 2016. 10

[84] R. S. Morris, D. Milia, J. Glover, L. M. Napolitano, B. Chen, E. Lindemann, M. R. Hemmila, D. Stein, E. Kummerfeld, J. Chipman, et al. Predictors of elderly mortality after trauma: A novel outcome score. *Journal of trauma and acute care surgery*, 88(3):416–424, 2020. 10

[85] M. A. Myszczynska, P. N. Ojamies, A. M. Lacoste, D. Neil, A. Saffari, R. Mead, G. M. Hautbergue, J. D. Holbrook, and L. Ferraiuolo. Applications of machine learning to diagnosis and treatment of neurodegenerative diseases. *Nature Reviews Neurology*, 16(8):440–456, 2020. 8

[86] B. Neal, N. Chapman, and A. Patel. Managing the global burden of cardiovascular disease. *European Heart Journal Supplements*, 4(suppl_F):F2–F6, 2002. 28

[87] D. Nie, H. Zhang, E. Adeli, L. Liu, and D. Shen. 3d deep learning for multi-modal imaging-guided survival time prediction of brain tumor patients. In *International conference on medical image computing and computer-assisted intervention*, pages 212–220. Springer, 2016. 9

[88] O. Oktay, J. Schlemper, L. L. Folgoc, M. Lee, M. Heinrich, K. Misawa, K. Mori, S. McDonagh, N. Y. Hammerla, B. Kainz, et al. Attention u-net: Learning where to look for the pancreas. *arXiv preprint arXiv:1804.03999*, 2018. 18, 22, 34

[89] A. H. Orabi, P. Buddhitha, M. H. Orabi, and D. Inkpen. Deep learning for depression detection of twitter users. In *Proceedings of the Fifth Workshop on Computational Linguistics and Clinical Psychology: From Keyboard to Clinic*, pages 88–97, 2018. 8

[90] M. Pahar, M. Klopper, R. Warren, and T. Niesler. Covid-19 cough classification using machine learning and global smartphone recordings. *Computers in Biology and Medicine*, page 104572, 2021. 12

[91] M. Pahar and T. Niesler. Machine learning based covid-19 detection from smartphone recordings: Cough, breath and speech. *arXiv preprint arXiv:2104.02477*, 2021. 12

[92] K. Pan, G. Hurault, K. Arulkumaran, H. C. Williams, and R. J. Tanaka. Eczemanet: Automating detection and severity assessment of atopic dermatitis. In *International Workshop on Machine Learning in Medical Imaging*, pages 220–230. Springer, 2020. 7

[93] M. Panahiazar, V. Taslimitehrani, N. Pereira, and J. Pathak. Using ehrs and machine learning for heart failure survival analysis. *Studies in health technology and informatics*, 216:40, 2015. 1

[94] D. G. Pankratz, Y. Choi, U. Imtiaz, G. M. Fedorowicz, J. D. Anderson, T. V. Colby, J. L. Myers, D. A. Lynch, K. K. Brown, K. R. Flaherty, et al. Usual interstitial pneumonia can be detected in transbronchial biopsies using machine learning. *Annals of the American Thoracic Society*, 14(11):1646–1654, 2017. 7

[95] R. B. Parikh, C. Manz, C. Chivers, S. H. Regli, J. Braun, M. E. Draugelis, L. M. Schuchter, L. N. Shulman, A. S. Navathe, M. S. Patel, et al. Machine learning approaches to predict 6-month mortality among patients with cancer. *JAMA network open*, 2(10):e1915997–e1915997, 2019. 9

[96] A. Paszke, S. Gross, F. Massa, A. Lerer, J. Bradbury, G. Chanan, T. Killeen, Z. Lin, N. Gimelshein, L. Antiga, A. Desmaison, A. Kopf, E. Yang, Z. DeVito, M. Raison, A. Tejani, S. Chilamkurthy, B. Steiner, L. Fang, J. Bai, and S. Chintala. Pytorch: An imperative style, high-performance deep learning library. In *Advances in Neural Information Processing Systems 32*, pages 8024–8035. Curran Associates, Inc., 2019. 19, 34

[97] G. Pinter, I. Felde, A. Mosavi, P. Ghamisi, and R. Gloaguen. Covid-19 pandemic prediction for hungary; a hybrid machine learning approach. *Mathematics*, 8(6):890, 2020. 12

[98] H. Porieva, K. Ivanko, C. Semkiv, and V. Vaityshyn. Investigation of lung sounds features for detection of bronchitis and copd using machine learning methods. *Visnyk NTUU KPI Seriia-Radiotekhnika Radioaparatobuduvannia*, (84):78–87, 2021. 7

[99] Z. Qu, Q. Liu, and C. Liu. Classification of congestive heart failure with different new york heart association functional classes based on heart rate variability indices and machine learning. *Expert Systems*, 36(3):e12396, 2019. 1, 6

[100] Y. Raita, T. Goto, M. K. Faridi, D. F. Brown, C. A. Camargo, and K. Hasegawa. Emergency department triage prediction of clinical outcomes using machine learning models. *Critical care*, 23(1):1–13, 2019. 10

[101] R. Rajaganeshan, C. Ludlam, D. Francis, S. Parasramka, and R. Sutton. Accuracy in ecg lead placement among technicians, nurses, general physicians and cardiologists. *International journal of clinical practice*, 62(1):65–70, 2008. 2, 14

[102] J. Rasheed, A. A. Hameed, C. Djeddi, A. Jamil, and F. Al-Turjman. A machine learning-based framework for diagnosis of covid-19 from chest x-ray images. *Interdisciplinary Sciences: Computational Life Sciences*, 13(1):103–117, 2021. 12

[103] S. V. Razavi-Termeh, A. Sadeghi-Niaraki, and S.-M. Choi. Asthma-prone areas modeling using a machine learning model. *Scientific Reports*, 11(1):1–16, 2021. 7

[104] A. H. Ribeiro, D. Gedon, D. M. Teixeira, M. H. Ribeiro, A. L. P. Ribeiro, T. B. Schön, and W. Meira. Automatic 12-lead ecg classification using a convolutional network ensemble. In *2020 Computing in Cardiology*, pages 1–4. IEEE, 2020. 24

[105] C. Rizzo, F. Monitillo, and M. Iacoviello. 12-lead electrocardiogram features of arrhythmic risk: A focus on early repolarization. *World Journal of Cardiology*, 8(8):447, 2016. 2, 14

[106] O. Ronneberger, P. Fischer, and T. Brox. U-net: Convolutional networks for biomedical image segmentation. In *Medical Image Computing and Computer-Assisted Intervention–MICCAI 2015: 18th International Conference, Munich, Germany, October 5-9, 2015, Proceedings, Part III 18*, pages 234–241. Springer, 2015. 29, 34

[107] V. Rowtula, S. Oota, M. Gupta, and B. R. Surampudi. A deep autoencoder for near-perfect fmri encoding. 2018. 8

[108] H. Rumpold, D. Niedersüß-Beke, C. Heiler, D. Falch, H. V. Wundsam, S. Metz-Gercek, G. Piringer, and J. Thaler. Prediction of mortality in metastatic colorectal cancer in a real-life population: a multicenter explorative analysis. *BMC cancer*, 20(1):1–9, 2020. 9

[109] S. Russell and P. Norvig. Artificial intelligence: a modern approach. 2002. 4

[110] J. R. Sato, J. Moll, S. Green, J. F. Deakin, C. E. Thomaz, and R. Zahn. Machine learning algorithm accurately detects fmri signature of vulnerability to major depression. *Psychiatry Research: Neuroimaging*, 233(2):289–291, 2015. 8

[111] R. W. Schafer. What is a savitzky-golay filter?[lecture notes]. *IEEE Signal processing magazine*, 28(4):111–117, 2011. 17

[112] R. M. Scheffler, J. X. Liu, Y. Kinfu, and M. R. Dal Poz. Forecasting the global shortage of physicians: an economic-and needs-based approach. *Bulletin of the World Health Organization*, 86:516–523B, 2008. 1, 4

[113] Z. K. Senturk. Early diagnosis of parkinson's disease using machine learning algorithms. *Medical hypotheses*, 138:109603, 2020. 8

[114] L. Serviá, N. Montserrat, M. Badia, J. A. Llompart-Pou, J. A. Barea-Mendoza, M. Chico-Fernández, M. Sánchez-Casado, J. M. Jiménez, D. M. Mayor, and J. Trujillano. Machine learning techniques for mortality prediction in critical traumatic patients: anatomic and physiologic variables from the retrauci study. *BMC Medical Research Methodology*, 20(1):1–12, 2020. 10

[115] L. D. Sharma and R. K. Sunkaria. Inferior myocardial infarction detection using stationary wavelet transform and machine learning approach. *Signal, Image and Video Processing*, 12(2):199–206, 2018. 1, 6

[116] R. L. Siegel, K. D. Miller, and A. Jemal. Cancer statistics, 2019. *CA: a cancer journal for clinicians*, 69(1):7–34, 2019. 9

[117] L. A. V. Silva and K. Rohr. Pan-cancer prognosis prediction using multimodal deep learning. In *2020 IEEE 17th International Symposium on Biomedical Imaging (ISBI)*, pages 568–571. IEEE, 2020. 9

[118] S. Simpraga, R. Alvarez-Jimenez, H. D. Mansvelder, J. M. Van Gerven, G. J. Groeneveld, S.-S. Poil, and K. Linkenkaer-Hansen. Eeg machine learning for accurate detection of cholinergic intervention and alzheimer's disease. *Scientific reports*, 7(1):1–11, 2017. 8

[119] P. K. Singh and C. M. Krishna. Continuum arm robotic manipulator: A review. *Universal Journal of Mechanical Engineering*, 2(6):193–198, 2014. 11

[120] J. Sohn, S. Yang, J. Lee, Y. Ku, and H. C. Kim. Reconstruction of 12-lead electrocardiogram from a three-lead patch-type device using a lstm network. *Sensors*, 20(11):3278, 2020. 15

[121] D. Spathis and P. Vlamos. Diagnosing asthma and chronic obstructive pulmonary disease with machine learning. *Health informatics journal*, 25(3):811–827, 2019. 7

[122] L. Steardo Jr, E. A. Carbone, R. de Filippis, C. Pisanu, C. Segura-Garcia, A. Squassina, P. De Fazio, and L. Steardo. Application of support vector machine on fmri data as biomarkers in schizophrenia diagnosis: A systematic review. *Frontiers in Psychiatry*, 11:588, 2020. 8

[123] S. G. Surampudi, S. Naik, R. B. Surampudi, V. K. Jirsa, A. Sharma, and D. Roy. Multiple kernel learning model for relating structural and functional connectivity in the brain. *Scientific reports*, 8(1):1–14, 2018. 8

[124] B. Surawicz and T. Knilans. *Chou's electrocardiography in clinical practice: adult and pediatric*. Elsevier Health Sciences, 2008. 2, 14, 28

[125] A. J. Sweatt, H. K. Hedlin, V. Balasubramanian, A. Hsi, L. K. Blum, W. H. Robinson, F. Haddad, P. M. Hickey, R. Condliffe, A. Lawrie, et al. Discovery of distinct immune phenotypes using machine learning in pulmonary arterial hypertension. *Circulation research*, 124(6):904–919, 2019. 7

[126] A. J. Swift, H. Lu, J. Uthoff, P. Garg, M. Cogliano, J. Taylor, P. Metherall, S. Zhou, C. S. Johns, S. Alabed, et al. A machine learning cardiac magnetic resonance approach to extract disease features and automate pulmonary arterial hypertension diagnosis. *European Heart Journal-Cardiovascular Imaging*, 22(2):236–245, 2021. 7

[127] S. Tabibu, P. Vinod, and C. Jawahar. Pan-renal cell carcinoma classification and survival prediction from histopathology images using deep learning. *Scientific reports*, 9(1):1–9, 2019. 8

[128] A. Tagaris, D. Kollias, A. Stafylopatis, G. Tagaris, and S. Kollias. Machine learning for neurodegenerative disorder diagnosis—survey of practices and launch of benchmark dataset. *International Journal on Artificial Intelligence Tools*, 27(03):1850011, 2018. 8

[129] W. Tang, Y. Cao, and X. Ma. Novel prognostic prediction model constructed through machine learning on the basis of methylation-driven genes in kidney renal clear cell carcinoma. *Bioscience reports*, 40(7):BSR20201604, 2020. 9

[130] M. P. Than, J. W. Pickering, Y. Sandoval, A. S. Shah, A. Tsanas, F. S. Apple, S. Blankenberg, L. Cullen, C. Mueller, J. T. Neumann, et al. Machine learning to predict the likelihood of acute myocardial infarction. *Circulation*, 140(11):899–909, 2019. 1, 6

[131] M. Toğaçar, B. Ergen, Z. Cömert, and F. Özyurt. A deep feature learning model for pneumonia detection applying a combination of mrmr feature selection and machine learning models. *Irbm*, 41(4):212–222, 2020. 7

[132] Y. J. Trakadis, S. Sardaar, A. Chen, V. Fulginiti, and A. Krishnan. Machine learning in schizophrenia genomics, a case-control study using 5,090 exomes. *American Journal of Medical Genetics Part B: Neuropsychiatric Genetics*, 180(2):103–112, 2019. 8

[133] P. Tschandl, N. Codella, B. N. Akay, G. Argenziano, R. P. Braun, H. Cabo, D. Gutman, A. Halpern, B. Helba, R. Hofmann-Wellenhof, et al. Comparison of the accuracy of human readers versus machine-learning algorithms for pigmented skin lesion classification: an open, web-based, international, diagnostic study. *The Lancet Oncology*, 20(7):938–947, 2019. 7

[134] K. D. Tzimourta, V. Christou, A. T. Tzallas, N. Giannakeas, L. G. Astrakas, P. Angelidis, D. Tsalikakis, and M. G. Tsipouras. Machine learning algorithms and statistical approaches for alzheimer's disease analysis based on resting-state eeg recordings: A systematic review. *International Journal of Neural Systems*, pages 2130002–2130002, 2021. 8

[135] A. Udrea, G. Mitra, D. Costea, E. Noels, M. Wakkee, D. Siegel, T. de Carvalho, and T. Nijsten. Accuracy of a smartphone application for triage of skin lesions based on machine learning algorithms. *Journal of the European Academy of Dermatology and Venereology*, 34(3):648–655, 2020. 7

[136] S. Umapathy, M. Sampath, S. Srivastava, et al. Automated segmentation and classification of psoriasis hand thermal images using machine learning algorithm. In *Proceedings of the International e-Conference on Intelligent Systems and Signal Processing*, pages 487–496. Springer, 2022. 7

[137] A. R. Vaka, B. Soni, and S. Reddy. Breast cancer detection by leveraging machine learning. *ICT Express*, 6(4):320–324, 2020. 8

[138] A. Vaswani, N. Shazeer, N. Parmar, J. Uszkoreit, L. Jones, A. N. Gomez, Ł. Kaiser, and I. Polosukhin. Attention is all you need. *Advances in neural information processing systems*, 30, 2017. 40

[139] T. Vijayakumar. Classification of brain cancer type using machine learning. *Journal of Artificial Intelligence*, 1(02):105–113, 2019. 8

[140] P. Virtanen, R. Gommers, T. E. Oliphant, M. Haberland, T. Reddy, D. Cournapeau, E. Burovski, P. Peterson, W. Weckesser, J. Bright, et al. Scipy 1.0: fundamental algorithms for scientific computing in python. *Nature methods*, 17(3):261–272, 2020. 30

[141] R. Vivanco and D. Roberts. Predicting patients likely to overstay in hospitals. In *2011 10th International Conference on Machine Learning and Applications and Workshops*, volume 2, pages 168–171. IEEE, 2011. 11

[142] K. Vo, E. K. Naeini, A. Naderi, D. Jilani, A. M. Rahmani, N. Dutt, and H. Cao. P2e-wgan: Ecg waveform synthesis from ppg with conditional wasserstein generative adversarial networks. In *Proceedings of the 36th Annual ACM Symposium on Applied Computing*, pages 1030–1036, 2021. 29, 38

[143] P. Wagner, N. Strodthoff, R.-D. Bousseljot, D. Kreiseler, F. I. Lunze, W. Samek, and T. Schaeffter. Ptb-xl, a large publicly available electrocardiography dataset. *Scientific data*, 7(1):1–15, 2020. 17

[144] N. Wan, D. Weinberg, T.-Y. Liu, K. Niehaus, E. A. Ariazi, D. Delubac, A. Kannan, B. White, M. Bailey, M. Bertin, et al. Machine learning enables detection of early-stage colorectal cancer by whole-genome sequencing of plasma cell-free dna. *BMC cancer*, 19(1):1–10, 2019. 8

[145] C. Wang, Y. Zhao, B. Jin, X. Gan, B. Liang, Y. Xiang, X. Zhang, Z. Lu, and F. Zheng. Development and validation of a predictive model for coronary artery disease using machine learning. *Frontiers in Cardiovascular Medicine*, 8:43, 2021. 1, 6

[146] D. Wang, J. Mo, G. Zhou, L. Xu, and Y. Liu. An efficient mixture of deep and machine learning models for covid-19 diagnosis in chest x-ray images. *PloS one*, 15(11):e0242535, 2020. 12

[147] K. Wang, P. Zuo, Y. Liu, M. Zhang, X. Zhao, S. Xie, H. Zhang, X. Chen, and C. Liu. Clinical and laboratory predictors of in-hospital mortality in patients with coronavirus disease-2019: a cohort study in wuhan, china. *Clinical infectious diseases*, 71(16):2079–2088, 2020. 12

[148] L.-d. Wang, W. Zhou, Y. Xing, N. Liu, M. Movahedipour, and X.-g. Zhou. A novel method based on convolutional neural networks for deriving standard 12-lead ecg from serial 3-lead ecg. *Frontiers of Information Technology & Electronic Engineering*, 20(3):405–413, 2019. 15

[149] P. Wang, X. Zheng, J. Li, and B. Zhu. Prediction of epidemic trends in covid-19 with logistic model and machine learning technics. *Chaos, Solitons & Fractals*, 139:110058, 2020. 12

[150] Z. Wang, Y. Zhu, D. Li, Y. Yin, and J. Zhang. Feature rearrangement based deep learning system for predicting heart failure mortality. *Computer methods and programs in biomedicine*, 191:105383, 2020. 10

[151] J. C. Weiss, S. Natarajan, P. L. Peissig, C. A. McCarty, and D. Page. Machine learning for personalized medicine: predicting primary myocardial infarction from electronic health records. *Ai Magazine*, 33(4):33–33, 2012. 1, 6

[152] M. Wheeler. Overview on robotics in the laboratory. *Annals of clinical biochemistry*, 44(3):209–218, 2007. 11

[153] M. Wijnberge, J. Schenk, L. Terwindt, M. Mulder, M. Hollmann, A. Vlaar, D. Veelo, and B. Geerts. The use of a machine-learning algorithm that predicts hypotension during surgery in combination with personalized treatment guidance: study protocol for a randomized clinical trial. *Trials*, 20(1):1–9, 2019. 11

[154] K. Xu, C. Li, J. Zhu, and B. Zhang. Understanding and stabilizing gans' training dynamics using control theory. In *International Conference on Machine Learning*, pages 10566–10575. PMLR, 2020. 16

[155] A. Yala, R. Barzilay, L. Salama, M. Griffin, G. Sollender, A. Bardia, C. Lehman, J. M. Buckley, S. B. Coopey, F. Polubriaginof, et al. Using machine learning to parse breast pathology reports. *Breast cancer research and treatment*, 161(2):203–211, 2017. 11

[156] G.-W. Yoon, S. Joo, C. Kyungmin, and H.-C. Seo. Chest-lead generation with single-lead. 2022 Computing in Cardiology. 16, 22

[157] Q. Yuan, T. Cai, C. Hong, M. Du, B. E. Johnson, M. Lanuti, T. Cai, and D. C. Christiani. Performance of a machine learning algorithm using electronic health record data to identify and estimate survival in a longitudinal cohort of patients with lung cancer. *JAMA Network Open*, 4(7):e2114723–e2114723, 2021. 9

[158] P. S. Zarrin, N. Roeckendorf, and C. Wenger. In-vitro classification of saliva samples of copd patients and healthy controls using machine learning tools. *IEEE Access*, 8:168053–168060, 2020. 7

[159] L. Zhang. Eeg signals classification using machine learning for the identification and diagnosis of schizophrenia. In *2019 41st Annual International Conference of the IEEE Engineering in Medicine and Biology Society (EMBC)*, pages 4521–4524. IEEE, 2019. 8

[160] M. Zhou, H. Zhao, X. Wang, J. Sun, and J. Su. Analysis of long noncoding rnas highlights region-specific altered expression patterns and diagnostic roles in alzheimer's disease. *Briefings in bioinformatics*, 20(2):598–608, 2019. 8

[161] Z. Zhou, M. M. Rahman Siddiquee, N. Tajbakhsh, and J. Liang. Unet++: A nested u-net architecture for medical image segmentation. In *Deep Learning in Medical Image Analysis and Multimodal Learning for Clinical Decision Support: 4th International Workshop, DLMIA 2018, and 8th International Workshop, ML-CDS 2018, Held in Conjunction with MICCAI 2018, Granada, Spain, September 20, 2018, Proceedings 4*, pages 3–11. Springer, 2018. 34

[162] H. Zhu, Y. Pan, K.-T. Cheng, and R. Huan. A lightweight piecewise linear synthesis method for standard 12-lead ecg signals based on adaptive region segmentation. *PloS one*, 13(10):e0206170, 2018. 15

[163] Q. Zhu, X. Tian, C.-W. Wong, and M. Wu. Ecg reconstruction via ppg: A pilot study. In *2019 IEEE EMBS international conference on biomedical & health informatics (BHI)*, pages 1–4. IEEE, 2019. 29

[164] Y. Zoabi, S. Deri-Rozov, and N. Shomron. Machine learning-based prediction of covid-19 diagnosis based on symptoms. *npj digital medicine*, 4(1):1–5, 2021. 12